JGR Atmospheres

RESEARCH ARTICLE
10.1029/2020JD033225

Key Points:
- Arctic MSA and non-sea-salt sulfate concentrations show increasing summer trends over the past two decades (2.5% and 2.1%) at Utqiaġvik, AK
- Concentrations of MSA at Oliktok Point are highly correlated to temperature as air masses are consistently from the Beaufort Sea
- Summers with Arctic cyclones have better correlation of MSA with ambient temperature

Supporting Information:
- Supporting Information S1

Correspondence to:
R. J. Sheesley,
Rebecca_Sheesley@baylor.edu

Citation:
Moffett, C. E., Barrett, T. E., Liu, J., Gunsch, M. J., Upchurch, L. M., Quinn, P. K., et al. (2020). Long-term trends for marine sulfur aerosol in the Alaskan Arctic and relationships with temperature. *Journal of Geophysical Research: Atmospheres*, *125*, e2020JD033225. https://doi.org/10.1029/2020JD033225

Received 9 JUN 2020
Accepted 5 OCT 2020
Accepted article online 24 OCT 2020

Author Contributions:
Conceptualization: Claire E. Moffett, Kerri A. Pratt, Rebecca J. Sheesley
Data curation: Lucia M. Upchurch, Patricia K. Quinn, Kerri A. Pratt
Formal analysis: Claire E. Moffett, Tate E. Barrett, Jun Liu, Matthew J. Gunsch, Lucia M. Upchurch, Patricia K. Quinn
Funding acquisition: Claire E. Moffett, Kerri A. Pratt, Rebecca J. Sheesley
Investigation: Claire E. Moffett, Tate E. Barrett, Jun Liu, Matthew J. Gunsch, Lucia M. Upchurch, Patricia K. Quinn, Kerri A. Pratt
Methodology: Claire E. Moffett, Tate E. Barrett
Project administration: Claire E. Moffett, Patricia K. Quinn, Kerri A. Pratt, Rebecca J. Sheesley
(continued)

Long-Term Trends for Marine Sulfur Aerosol in the Alaskan Arctic and Relationships With Temperature

Claire E. Moffett[1], Tate E. Barrett[1,2,3], Jun Liu[4], Matthew J. Gunsch[4,5], Lucia M. Upchurch[6,7], Patricia K. Quinn[7], Kerri A. Pratt[4], and Rebecca J. Sheesley[1,2]

[1]Department of Environmental Science, Baylor University, Waco, TX, USA, [2]The Institute of Ecological, Earth, and Environmental Sciences, Baylor University, Waco, TX, USA, [3]Now at Barrett Environmental, McKinney, TX, USA, [4]Department of Chemistry, University of Michigan, Ann Arbor, MI, USA, [5]Now at Merck & Co., Inc., Kenilworth, NJ, USA, [6]Joint Institute for the Study of the Atmosphere and Ocean, University of Washington, Seattle, WA, USA, [7]Pacific Marine Environmental Laboratories, National Oceanic and Atmospheric Administration, Seattle, WA, USA

Abstract Marine aerosol plays a vital role in cloud-aerosol interactions during summer in the Arctic. The recent rise in temperature and decrease in sea ice extent have the potential to impact marine biogenic sources. Compounds like methanesulfonic acid (MSA) and non-sea-salt sulfate (nss-SO_4^{2-}), oxidation products of dimethyl sulfide (DMS) emitted by marine primary producers, are likely to increase in concentration. Long-term studies are vital to understand these changes in marine sulfur aerosol and potential interactions with Arctic climate. Samples were collected over three summers at two coastal sites on the North Slope of Alaska (Utqiaġvik and Oliktok Point). MSA concentrations followed previously reported seasonal trends, with evidence of high marine primary productivity influencing both sites. When added to an additional data set collected at Utqiaġvik, an increase in MSA concentration of + 2.5% per year and an increase in nss-SO_4^{2-} of + 2.1% per year are observed for the summer season over the 20-year record (1998–2017). This study identifies ambient air temperature as a strong factor for MSA, likely related to a combination of interrelated factors including warmer sea surface temperature, reduced sea ice, and temperature-dependent chemical reactions. Analysis of individual particles at Oliktok Point, within the North Slope of Alaska oil fields, showed evidence of condensation of MSA onto anthropogenic particles, highlighting the connection between marine and oil field emissions and secondary organic aerosol. This study shows the continued importance of understanding MSA in the Arctic while highlighting the need for further research into its seasonal relationship with organic carbon.

Plain Language Summary Particles in the Earth's atmosphere play an important role in affecting the planet's climate. Understanding the compounds that make up these aerosol particles is especially important in the Arctic where dramatic changes in temperature and sea ice extent are being observed. Aerosol resulting from biological activity in marine regions is expected to increase in concentration and therefore have greater effects on climate. Methanesulfonic acid is one such compound that can be utilized to understand the impact of marine aerosol sources. Aerosol samples were collected over three summers at two sites on the North Slope of Alaska: Utqiaġvik and Oliktok Point. The samples were analyzed for a wide range of compounds including methanesulfonic acid. The results were combined with 16 years of data from the National Oceanic and Atmospheric Administration. Concentrations of methanesulfonic acid are increasing at a rate of 2.5% per year. Methanesulfonic acid was strongly related to temperature at Oliktok Point, where most marine aerosol is from the Beaufort Sea. At Utqiaġvik, strong relationships were found between methanesulfonic acid and temperature during years when intense Arctic cyclones occurred.

1. Introduction

Aerosol particles in the Earth's atmosphere can have direct and indirect effects on the planet's radiative budget including absorbing and scattering light as well as acting as cloud condensation nuclei (CCN) (Chen & Bond, 2010; Williams et al., 2001). The composition, concentration, and particle size will determine how effective the aerosol will be as CCN (Dusek et al., 2006; McFiggans et al., 2005; Petters &

Resources: Claire E. Moffett, Rebecca J. Sheesley
Supervision: Claire E. Moffett, Kerri A. Pratt, Rebecca J. Sheesley
Visualization: Claire E. Moffett, Tate E. Barrett, Jun Liu, Matthew J. Gunsch
Writing - original draft: Claire E. Moffett, Tate E. Barrett, Jun Liu, Matthew J. Gunsch
Writing – review & editing: Claire E. Moffett, Tate E. Barrett, Jun Liu, Matthew J. Gunsch, Lucia M. Upchurch, Patricia K. Quinn, Kerri A. Pratt, Rebecca J. Sheesley

Kreidenweis, 2007). Larger particles are typically always CCN active despite their composition, while the addition of soluble material to an insoluble particle can increase its CCN ability (Dusek et al., 2006). The ability of aerosol to act as CCN can be measured using the hygroscopicity parameter kappa (κ) (Petters & Kreidenweis, 2007). Inorganic compounds, such as sea salt, have higher κ, indicating that they are more efficient CCN. For complex atmospheric aerosol an average κ can be calculated. Changes in the organic fraction of aerosol have the potential to alter this CCN activity and therefore influence the Earth's radiative budget (Leck et al., 2002; Martin et al., 2011; Petters & Kreidenweis, 2007).

The composition and effects of aerosol are extremely important to understand in the Arctic, which is warming faster than any other region of the world (Stocker, 2014). Long-range transport from lower latitudes can be an important source of aerosol; however, in the summertime wet removal results in less efficient transport of aerosol, meaning that the Arctic atmosphere can be characterized as relatively clean near the surface (Croft et al., 2016; Di Pierro et al., 2013; Polissar et al., 1999). In periods with no influence from transport, aerosol numbers are strongly influenced by new particle formation and growth (NPF/G), which has been shown to control the concentration of CCN in the Arctic (Croft et al., 2016; Heintzenberg et al., 2017; Köllner et al., 2017; Leaitch et al., 2013; Willis et al., 2017). Emissions of dimethyl sulfide (DMS) released by phytoplankton can be influential in these processes. Studies have shown that oxidation products of DMS can control the formation of ultrafine particles in the clean summertime atmosphere, which can then grow large enough to act as CCN (Abbatt et al., 2019; Ghahremaninezhad et al., 2019; Leaitch et al., 2013; Nilsson & Leck, 2002; Pandis et al., 1994; Park et al., 2017; Rempillo et al., 2011). DMS is oxidized in the atmosphere to form sulfate and methanesulfonic acid (MSA) (Hatakeyama et al., 1985; Leaitch et al., 2013). Summertime MSA and sulfate concentrations were demonstrated to be increasing in the Arctic from the late 1990s to the early 2000s, a trend that has been attributed to changes in the Arctic such as warmer temperatures and decreased sea ice extent (Breider et al., 2017; Laing et al., 2013; Polissar et al., 1999; Quinn et al., 2009). Values of κ for various common methanesulfonates have been reported ranging from 0.30 to 0.38 for calcium methanesulfonate, 0.46 for sodium methanesulfonate, and 0.47 for potassium methanesulfonate (Tang et al., 2015, 2019). For sulfate, κ's have been reported of 0.61 for $(NH_4)_2SO_4$ to 0.90 for H_2SO_4 (Clegg et al., 1998; Petters & Kreidenweis, 2007). Aerosol with higher concentrations of sulfate compared to MSA will be more CCN active (Leaitch et al., 2013). Aerosol components resulting from NPF/G, specifically those from marine sources (i.e., DMS), are essential to study in order to understand the effects of aerosol on the Arctic climate. While sulfate can have additional sources in the atmosphere including volcanic, terrestrial, and anthropogenic origins, MSA is solely produced from the oxidation of DMS, making it ideal to study trends in marine aerosol and how it may be affected by changes in the Arctic climate.

As the Arctic warms, sea ice extent and seasonality have large implications for future aerosol composition, specifically aerosol resulting from marine sources such as MSA and sulfate (Browse et al., 2014). The two coastal sites chosen for this study, Utqiaġvik, AK, and Oliktok Point, AK, both are heavily influenced by marine sources (Figure 1). This makes them ideal locations to study the impact of marine sulfur aerosol on the North Slope of Alaska (NSA) as well as differences in aerosol composition over time.

Long-term studies of MSA have shown that it has a distinct seasonal cycle with a large peak in the spring followed by a smaller peak in the late summer (Leck & Persson, 1996; Li et al., 1993; Sharma et al., 2019). As ice disappears earlier, the start of the high productivity season has shifted earlier in the year while the end has become delayed (Kahru et al., 2011, 2016). Melt ponds over ice have also been reported to have high concentrations of DMS and will likely become more important as ice decreases and becomes younger (Abbatt et al., 2019; Gourdal et al., 2018; Mungall et al., 2016). The continued decrease in ice extent will likely result in higher net primary productivity, increased DMS emissions, and changes in the seasonal cycle of MSA (Galí et al., 2019; Renaut et al., 2018). Model studies also suggest that DMS emissions will increase in an ice-free Arctic Ocean during the summer months as well as with the continued thinning of sea ice (Browse et al., 2014; Renaut et al., 2018). A study of the relationship between MSA and sea ice extent and area over 8 years in Ny Ålesund, Svalbard, and Thule, Greenland, found that MSA concentrations increased with decreasing sea ice extent and area during the spring while there was less significant or no relationship between them in the summer (Becagli et al., 2019). Increasing cloudiness in the Arctic could potentially have negative effects on primary productivity and therefore MSA concentrations (Bélanger et al., 2013). Concentrations of MSA have also been shown to be associated with sea surface temperature (Laing et al., 2013; Ye et al., 2015). Trends in MSA and sulfate have been previously studied at Utqiaġvik over a 10-year period, and researchers discussed

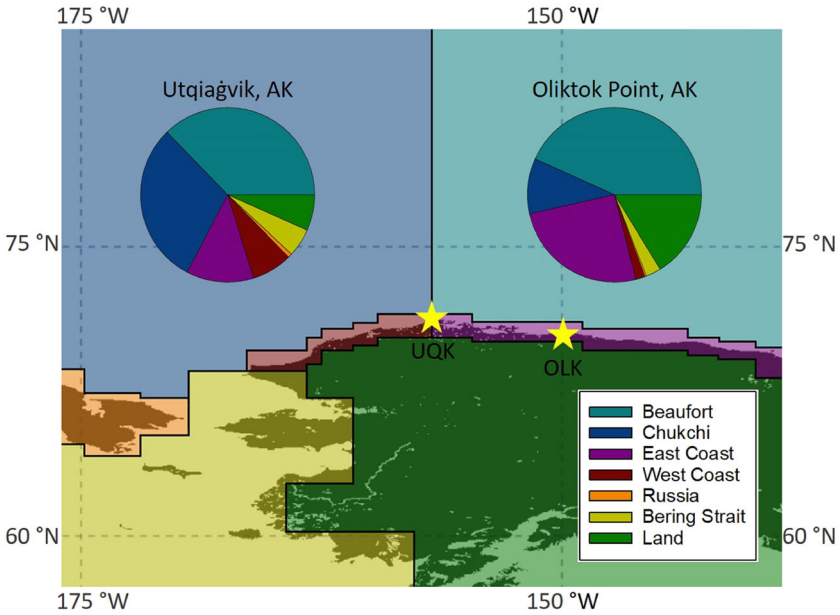

Figure 1. A map depicting the geographical identifications used for 48-hr backward air mass trajectory percentage calculations (section 2.4), with the two coastal sampling sites starred: Utqiaġvik (UQK) and Oliktok (OLK). The pie charts display the average percentage contributions of air masses from the different geographic areas over all sampling periods (summers in 2015, 2016, and 2017) for the 48-hr back trajectories.

possible effects of parameters such as sea ice extent and sea surface temperature on the concentrations (O'Dwyer et al., 2000; Quinn et al., 2009; Sharma et al., 2012). The current study combines results from that original study, an additional 6 years of National Oceanic and Atmospheric Administration (NOAA) data, and the results from the synoptic NSA study to produce 20-year trends for Utqiaġvik.

Decreasing ice extent, as well as increased temperatures, is associated with a general increase in the occurrence and intensity of cyclones in the Arctic (Serreze & Barrett, 2008; Serreze et al., 2000; Zhang et al., 2014). High winds from storms and cyclones create vertical mixing in surface water, bringing nutrients to the sea surface microlayer (SML) and increasing phytoplankton activity. The Great Arctic Cyclone of August 2012, which covered areas of the Arctic Ocean from Northern Siberia to the Canadian Archipelago, had effects on primary productivity which were especially noticeable in the Bering Strait region (Simmonds & Rudeva, 2012; Zhang et al., 2014). It is likely that the Extreme Arctic Cyclone of August 2016, which lasted for over a month and at one point covered the entire Pacific region of the Arctic Ocean, had similar results on phytoplankton activity (Yamagami et al., 2017). Synoptic measurement efforts for the current study included summer sampling in 2015, 2016, and 2017, so possible effects from the cyclone in 2016 may be reflected in the samples.

This study evaluates whether previous long-term increases in MSA and sulfate at Utqiaġvik have continued by expanding summer measurements to nearly two decades of data. Possible influences on MSA concentration are considered including short-term changes in ambient temperature and cyclonic activity. Utqiaġvik allows for an understanding of the state of MSA at a site of mixed marine aerosol source regions including the Beaufort and Chukchi Seas. The addition of another site, Oliktok Point, improves characterization of marine biogenic aerosol from the Beaufort Sea. At this site, the composition of individual MSA-containing particles was also examined using single-particle mass spectrometry. The goal of this paper is to study trends in MSA over time at two sites on the NSA and explore additional influences on its concentration as it relates to the changing Arctic.

2. Methods

2.1. Field Collection

Atmospheric particulate matter (PM) samples were collected for a synoptic campaign at two sites on the NSA over three summers (2015, 2016, and 2017) during two Department of Energy Atmospheric Radiation

Measurement (DOE ARM) field campaigns. The first site is the permanent DOE ARM NSA Climate Research Facility, 7.4 km northeast of the village of Utqiaġvik (UQK), Alaska (71°19′23.73″N, 156°36′56.70″W), which has a population of 4,438, and is 515 km north of the Arctic Circle. The site is approximately 1.6 km from the nearest coast. Using collocated BC and wind direction measurements, it has been demonstrated that the site receives minimal aerosol contribution from the village (Barrett et al., 2015). The second site is the DOE NSA ARM mobile facility (AMF3) at Oliktok Point (OLK), Alaska (70°29′42″N, 149°53′9.6″W). The site is 300 km southeast of Utqiaġvik, AK, in a region of intense petroleum development, 0.5 km from the nearest coast. Sampling occurred from August through September 2015 and June 2016 through September 2017 at both sites. Total suspended particulate (TSP) matter samples were collected during these two campaigns; detailed analysis of the summertime TSP is the focus of this paper.

TSP samples were collected on quartz fiber filters (QFFs; Tissuquartz Filters 2500 QAT-UP; 20 × 25 cm). Hi-Q high volume samplers customized with insulation for cold weather sampling (HVP-5300AFC; HI-Q Environmental Products Company, Inc., San Diego, CA 92121) were utilized. The samplers were elevated on platforms approximately 10 m above ground level. Flow rates were calibrated before and after the sampling campaigns. The Hi-Q high volume samplers were calibrated with a HI-Q D-AFC-Series air flow calibrator and an Auto Flow Calibration feature included on the samplers. For all three summers the sampling duration was on average 1 week at a flow rate of 1.2 m^3 min^{-1}. QFFs were baked prior to sampling at 500°C for 12 hr and stored in aluminum foil packets and storage bags in a freezer before and after sampling. Filter changes were performed on aluminum foil sheets that were baked for 12 hr at 500°C and stored in a −10°C freezer in storage bags. Field blanks were taken periodically throughout the sampling campaigns by placing an unsampled filter in a filter holder, placing it in the sampler momentarily, and then removing it and placing the filter in storage. Field blanks were treated in the same manner as sampled filters. Filters were shipped back to Baylor University for analysis in coolers with ice packs roughly every 3 months and at the end of the sampling campaigns. Remaining filter samples for the campaigns are archived in freezers at Baylor University. A manuscript is currently in preparation that will report bulk organic carbon (OC) and elemental carbon (EC) concentrations, radiocarbon abundance, and positive matrix factorization analysis of the samples.

Results from the ARM field campaigns were combined with the samples and analysis completed by NOAA for their site near Utqiaġvik (71°19′22.7994″N, 156°36′41.04″W). The Barrow Atmospheric Baseline Observatory site is co-located with the ARM NSA site. The data set utilized here includes summertime data from 1998 to 2013. The 1998–2007 results were published by Quinn et al. (2009), while the 2008–2013 results have not previously been published for MSA and sulfate. Collection was completed using a Berner-type multijet cascade impactor with aerodynamic D_{50} cutoff diameters of 10 and 1.0 μm. Additional details about sample collection can be found in Quinn et al. (2002). The samples were analyzed by ion chromatography (IC) using the method described in Quinn et al. (1998). The data and trends reported in Quinn et al. (2009) were for the submicron size range. In order to better collate the data from this study with the results from Quinn et al. (2009), only the submicron data from NOAA were utilized here. The compounds of interest here mainly occur in the submicron size fraction (Leck & Persson, 1996), so little difference is expected between the $PM_{1.0}$ and TSP samples. During the 1998–2013 time period, MSA in the supermicron size fraction accounted for only 2% on average of the total MSA. There are also small differences in methodology which could potentially affect comparisons between the NOAA and Baylor data sets including sector-controlled sampling excluding 130° to 360° from 1998 to 2013. The analysis of the long-term trends here assumes that these differences do not greatly affect or bias the conclusions.

2.2. Ion Chromatography

Summer PM samples were analyzed for inorganic anions and cations as well as low molecular weight organic acids using IC. Inorganic anions included nitrate, nitrite, chloride, sulfate, bromide, and fluoride. Organic acids of interest were malonate, malate, oxalate, phthalate, acetate, and MSA. Technically, methanesulfonate is the measured ion, as it is detected as an anion; however, following previous literature it will be referred to as MSA. Inorganic cations included sodium, potassium, magnesium, lithium, calcium, and ammonium. The QFF extraction was previously reported in Barrett and Sheesley (2014). Briefly, soluble ions on the QFF were extracted by sonication and centrifugation in 25 ml of deionized water (Barrett & Sheesley, 2014). Field blanks and filter blanks were extracted in the same manner and included with each

analysis, and calibration curve check standards were run frequently. Deionized water blanks were included before and after the calibration curve as well as in between samples and check standards.

A Dionex ICS-2100 Reagent Free Ion Chromatography System (Thermo Scientific Dionex, Waltham, MA 02451) was utilized for analysis of the inorganic anions and organic acids. A Dionex IonPac AG11-HC guard column (4 × 50 mm) was used to help with separation before a Dionex IonPac AS11-HC (4 × 250 mm) analytical column. An eluent gradient was utilized with a potassium hydroxide eluent generator. The mobile-phase flow rate was 1.5 ml min^{-1}, and the column temperature was set to 30°C. The eluent gradient was optimized from a Thermo Scientific application note in order to analyze inorganic anions and organic acids and mitigate issues with high chloride response on the detection of MSA (Christison et al., 2015). The eluent gradient was increased at a slower rate after MSA eluted so that the chloride would elute at a later retention time. The gradient was also adjusted to remain constant during oxalate elution to ensure an increase in background noise due to increased eluent concentration did not interfere with detection. The calibration curve comprised of seven to eight points starting from 0.1 to up to 50 mg/L. Standards for the inorganic anions were purchased from Thermo Scientific, organic acids standards were purchased from Sigma Aldrich (St. Louis, MO 63118), and the MSA standard was purchased from Inorganic Ventures (Christiansburg, VA 24073). All compounds in all samples either fell within the calibration curve range or were below the method detection limit (Supporting Information Table S1) with the exception of those with high concentrations of sodium and chloride. The method used to properly quantify those samples for sodium and chloride is described later.

For the inorganic cations, a Dionex Aquion system was utilized. The column was a Dionex IonPac CS12A (4 × 250 mm) with a Dionex IonPac CG12A (4 × 50 mm) guard column. The isocratic eluent was 20-mM MSA for 15 min. The 6-cation standard for the inorganic cations was purchased from Thermo Scientific. Cation analysis protocol parallels the anion analysis described above. The ICS-2100 and Aquion systems utilize the same autosampler. Water extracts were analyzed directly after extraction first on the ICS-2100 for inorganic anions and organic acids due to their potential to degrade and then on the Aquion system for the inorganic cations. For the analysis of chloride and sodium, which were found in extremely high concentrations due to the proximity to the coast, an aliquot of the extract was taken and diluted 10× with DI water in order to ensure accurate detection within calibration curve range.

Concentrations of non-sea-salt sulfate (nss-SO_4^{2-}), calcium (nss-Ca^{2+}), potassium (nss-K^+), and magnesium (nss-Mg^{2+}) were determined based on the results of IC analysis. The concentrations were calculated by utilizing Na^+ concentrations ([Na^+]), the concentration of the compound ([X]), and the mass ratio of that compound to sodium in sea water (k) (Equation 1) (Holland, 1978; Virkkula et al., 2006). The ratio utilized was 0.252 for nss-SO_4^{2-}, 0.03791 for nss-Ca^{2+}, 0.121 for nss-Mg^{2+}, and 0.03595 for nss-K^+ (Dickson & Goyet, 1994; Wagenbach et al., 1998). Some of these calculations resulted in negative values for this study. Previous studies in polar regions have also reported negative concentrations for nss-SO_4^{2-}, which are likely the result of depletion of nss-SO_4^{2-} (Norman et al., 1999; Quinn et al., 2002; Wagenbach et al., 1998). To correct these negative values, a linear regression of the nss-SO_4^{2-} concentrations calculated with $k = 0.252$ and Na^+ concentrations was performed. The slope of the regression was then added to 0.252 to obtain a new k value for Equation 1 (Wagenbach et al., 1998). Negative values were also obtained for nss-Ca^{2+}, nss-K^+, and nss-Mg^{2+} and were corrected using the same method. The corrected k values for Utqiaġvik were 0.177 for nss-SO_4^{2-}, 0.02915 for nss-K^+, 0.088 for nss-Mg^{2+}, and 0.01441 for nss-Ca^{2+}. For Oliktok Point, the corrected k values were 0.194 for nss-SO_4^{2-}, 0.02035 for nss-K^+ and 0.097 for nss-Mg^{2+}, and 0.01481 for nss-Ca^{2+}.

$$[\mathrm{nss}-X] = [X]_{total} - k[\mathrm{Na}^+] \quad (1)$$

Concentrations of sea-salt aerosol were calculated using Equation 2. The value of 1.47 represents the seawater mass ratio of ($Na^+ + K^+ + Mg^{2+} + Ca^{2+} + SO_4^{2-} + HCO_3^-$)/$Na^+$ (Holland, 1978). This study follows previously reported methods of sea-salt concentration calculations which do not include any Cl^- greater than the Cl^- to Na^+ sea water ratio of 1.8 (Giardi et al., 2016; May et al., 2016; Quinn et al., 2002). This prevents the inclusion of non-sea-salt compounds and allows for Cl^- depletion. It also assumes that all Na^+ is from sea water (Quinn et al., 2002). Mineral dust containing Na^+ was reported at Utqiaġvik during

September 2015; however, dust was a minor contributor (4–14%, by number) compared to sea-salt aerosol for 0.2–1.5 μm particles (Gunsch et al., 2017). At Oliktok Point, mineral dust containing Na^+ accounted for only 1%, by number, of the 0.07–1.6 μm size fraction (Gunsch et al., 2019). Only one sample at Utqiaġvik and one from Oliktok had a Cl^- to Na^+ ratio greater than 1.8.

$$[\text{sea salt}] = [Cl^-] + [Na^+] \times 1.47 \quad (2)$$

2.3. Aerosol Time-of-Flight Mass Spectrometry

From 22 August to 16 September 2016 at Oliktok Point, the size and chemical composition of 32,880 individual particles (0.07–1.6 μm, vacuum aerodynamic diameter) were measured, in real time, using an aerosol time-of-flight mass spectrometer (ATOFMS). Overall aerosol composition during the study was described by Gunsch et al. (2019); here, we focus on the composition of individual particles containing MSA. This ATOFMS is based on the design of Pratt et al. (2009). Briefly, particles were focused through an aerodynamic lens system, and the diameter of each individual particle was calculated based on its time of flight between two continuous wave lasers (50 mW 405 nm and 50 mW 488 nm). Particles were then desorbed and ionized by a 266-nm Nd:YAG pulsed laser and measured by a dual-polarity reflectron time-of-flight mass spectrometer, resulting in positive and negative ion mass spectra for each individual particle. ATOFMS individual particle mass spectra were imported and analyzed in FATES, a MATLAB (The MathWorks, Inc.) software toolkit (Sultana et al., 2017), and these mass spectra were clustered based on the presence and intensity of ion peaks using an ART-2a neural network algorithm (Song et al., 1999). The resulting clusters were grouped into individual particle types, based on the most likely *m/z* assignments, according to ion ratios and spectral identification from previous laboratory and field campaigns (Pratt & Prather, 2009). Particles were categorized into eight individual particle types: OC, OC-amine-sulfate, sea spray aerosol, EC, EC and OC (ECOC), biomass burning, mineral dust, and incineration particles (Gunsch et al., 2019). Particles containing MSA were identified by searching for relative peak areas above 0.01 at *m/z* −95 ($CH_3SO_3^-$) (Gaston et al., 2010). It is important to note, however, that this peak has interferences from other ions at *m/z* −95 (PO_4^- or $NaCl_2^-$). In order to exclude these interferences, particles containing *m/z* −79 (PO_3^-), −93 ($NaCl_2^-$), or −97 ($NaCl_2^-$) are not classified as "MSA-containing" based on these potential interferences. This limits the ability to evaluate nascent (chloride-containing) sea spray aerosol for MSA content.

2.4. Backward Air Mass Trajectory Analysis and Sea Ice Extent

Backward air mass trajectories were modeled using the NOAA Hybrid Single-Particle Lagrangian Integrated Trajectory (HYSPLIT) online model (Rolph et al., 2017; Stein et al., 2015) to determine the geographic source regions of air masses impacting the site. Forty-eight-hour back trajectories were calculated every 6 hr starting at the last day and ending on the first day for each sample. The vertical motion was set to "Model vertical velocity," and the height was set to 10 m above ground level. Ambient temperature data were also requested with each back trajectory. One-week back trajectories were also calculated using the parameters described above.

Since this study is interested in marine aerosol production, the trajectory analysis was structured to consider differences in potential marine production areas. To assess this for the NSA, residence time of backward air mass trajectories was mapped out into seven different regions (Beaufort Sea, Chukchi Sea, East Coast of the NSA, West Coast of the NSA, Russia, Bering Strait, and inland Alaska). The seven regions surrounding the sites were chosen to highlight potential source regions for marine primary productivity emissions (Figure 1). Satellite imagery of chlorophyll (https://oceancolor.gsfc.nasa.gov/cgi/browse.pl?sen=am) from the Visible and Infrared Imager/Radiometer Suite (VIIRS) on the Suomi National Polar-orbiting Partnership spacecraft was used to aid in the selection of regions (NASA, 2018). Trajectory end point files were downloaded from the HYSPLIT online model in order to obtain geographic coordinates. Coordinates from the back-trajectory end point files were utilized to calculate the percentage of each back trajectory that lay in each region for every PM sample. Additional regions were determined for the 1-week back trajectories (Figure S1). More information about these regions can be found in the Supporting Information Text S1 and in Figures S2 and S3.

Sea ice extent data were obtained from the National Snow and Ice Data Center (NSIDC). The Sea Ice Index data products were utilized which are derived from the Near-Real-Time DMSP SSMIS Daily Polar Gridded Sea Ice Concentrations and Nimbus-7 SSMR and DMSP SSM/I-SSMIS Passive Microwave Data Sea Ice

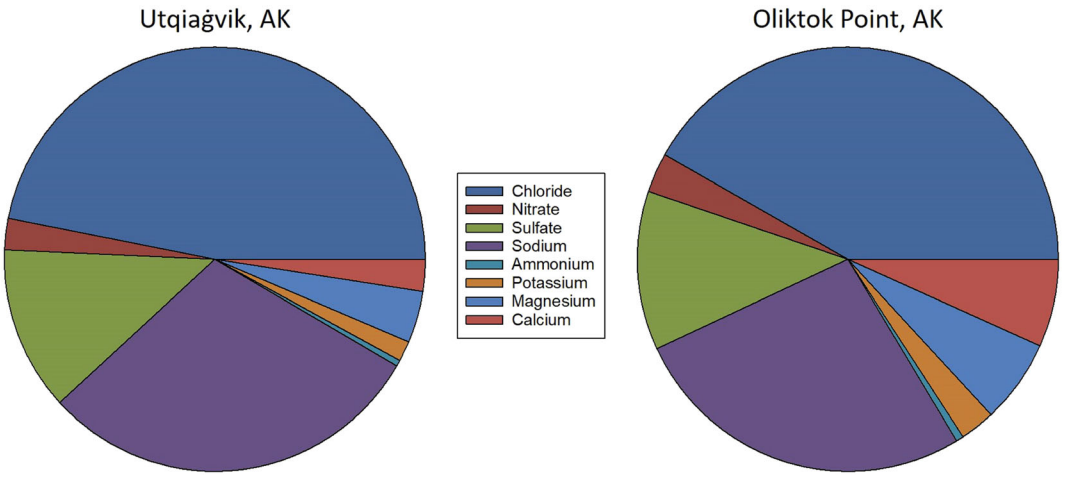

Figure 2. The average mass contribution of the major inorganic anions and cations for the summers of 2015–2017.

Concentrations. The monthly averages were selected for July, August, and September from 1998 to 2017 (Fetterer et al., 2017).

2.5. Statistical Analysis for Annual Trends

The nonparametric Mann-Kendall test, which assumes that there are no seasonal trends present in the data, was utilized to identify monotonic trends (Gilbert, 1987). The slope of the linear trends is estimated by the nonparametric Sen's method, which can be used when the assumed trend is linear (Sen, 1968). The Sen's method first calculates the slope between all data point pairs, with the slope estimate (Q) being the median of these data pair slopes (Salmi et al., 2002). Significance levels of $\alpha = 0.001$, 0.01, 0.05, and 0.1 are reported for the trends, where $\alpha < 0.1$ means that there is a probability of no trend being present of 10% or less. This method was selected in order to compare to previously reported trends (Quinn et al., 2009).

3. Results

3.1. Ionic Composition

Variability in the inorganic ion composition was assessed by site and by year (Figure 2 and Table 1). Both sites show a high influence of sea-salt aerosol (Figure 2). Sea-salt concentrations, calculated as described in the methods, varied between samples and did not have any obvious temporal patterns for the summer (Figure S4). Average concentrations of sea salt were similar for TSP across both sites in 2016 and 2017, while 2015 Utqiaġvik appears to have an overall higher average concentration, indicating greater influence of sea spray (Figure 1), although the wind speed was not significantly higher in 2015 (Table S2). Comparing averages for just the months of August–September, the difference in sea-salt concentrations is less between the summers, although still large between 2015 (2,700 ± 400 ng m^{-3}) and 2017 (1,800 ± 500 ng m^{-3}) (Table S3).

In addition to contribution from sea salt, Oliktok Point also had large contributions from ions such as total potassium, magnesium, and calcium compared to Utqiaġvik. In terms of potential sources, the roads surrounding each site are unpaved, leading to problems with road dust. The roads from Prudhoe Bay to Oliktok Point are used intensively for heavy equipment associated with oil and gas extraction/exploration and are maintained by the petroleum companies. The roads are periodically treated with salts such as K^+, Ca^{2+}, and Mg^{2+} chloride to control road dust (Withycombe & Dulla, 2006). ATOFMS measurements reported individual mineral dust particles containing Ca^{2+} and Mg^{2+} at Oliktok Point (August–September 2016) in the 0.07–1.6 μm size range (Gunsch et al., 2019). At Utqiaġvik (September 2015), ATOFMS data showed Ca^{2+}-rich and Fe^{+}-rich dust particles also attributed to nearby roads and beaches (Gunsch et al., 2017). Although biomass burning particles containing K^+ have also been observed at both sites, these were a minor contribution (Gunsch et al., 2017, 2019). The summer of 2015 at Oliktok had the highest concentrations of K^+ and Mg^{2+}, which were three to four times higher than 2017 (Table 1). This may be due to changes in industry upkeep of local roads or meteorological parameters such

Table 1
Average Concentrations and Standard Deviation of Select Inorganic Ions and Organic Acids Analyzed by Ion Chromatography

	Utqiaġvik, AK (ng m^{-3})			Oliktok Point, AK (ng m^{-3})		
Compound	2015[a]	2016	2017	2015[a]	2016	2017
Chloride	1,436 ± 217	901 ± 66	670 ± 63	817 ± 124	900 ± 55	641 ± 54
Nitrite	0.34 ± 0.06	0.29 ± 0.04	3.9 ± 0.5	0.09 ± 0.03	0.16 ± 0.03	4.8 ± 0.4
Bromide	2.8 ± 0.5	0.18 ± 0.02	2.3 ± 0.3	<MDL	2.4 ± 0.1	4.1 ± 0.3
Nitrate	20 ± 3	45 ± 4	61 ± 7	48 ± 9	49 ± 3	69 ± 6
Sulfate	250 ± 35	245 ± 16	240 ± 21	200 ± 30	234 ± 13	229 ± 17
Sodium	850 ± 128	562 ± 40	470 ± 43	530 ± 81	550 ± 33	435 ± 35
Ammonium	6 ± 1	8.8 ± 0.6	11 ± 1	25 ± 5	8 ± 1	6.7 ± 0.7
Potassium	30 ± 5	35 ± 3	25 ± 2	86 ± 13	63 ± 5	21 ± 2
Magnesium	90 ± 13	90 ± 7	55 ± 5	228 ± 35	141 ± 11	49 ± 4
Calcium	34 ± 5	65 ± 6	31 ± 3	204 ± 33	151 ± 11	62 ± 5
Acetate	0.18 ± 0.05	2.1 ± 0.2	<MDL	4.6 ± 0.7	2.3 ± 0.2	<MDL
Formate	0.7 ± 0.1	2.8 ± 0.2	<MDL	1.9 ± 0.3	2.1 ± 0.2	0.19 ± 0.03
Malate	0.34 ± 0.09	4.8 ± 0.4	14 ± 2	0.3 ± 0.1	4.0 ± 0.3	22 ± 2
Malonate	0.7 ± 0.2	2.9 ± 0.2	4.1 ± 0.4	<MDL	3.5 ± 0.3	9.4 ± 0.7
MSA	3.3 ± 0.5	19 ± 1	22 ± 2	7 ± 1	13.3 ± 0.8	14 ± 1
Oxalate	2.2 ± 0.4	9.1 ± 0.7	5.8 ± 0.8	<MDL	8.7 ± 0.9	11 ± 1
nss-SO_4^{2-}	96 ± 14	145 ± 10	160 ± 15	100 ± 15	127 ± 7	145 ± 12
nss-K^+	3.4 ± 0.6	15 ± 2	7.8 ± 0.7	67 ± 10	44 ± 4	5.2 ± 0.4
nss-Mg^{2+}	13 ± 2	36 ± 4	10 ± 1	164 ± 25	81 ± 8	6.2 ± 0.5
nss-Ca^{2+}	7 ± 2	44 ± 5	14 ± 2	184 ± 31	131 ± 10	46 ± 4
Sea salt	2,685 ± 405	1,725 ± 124	1,360 ± 127	1,596 ± 243	1,708 ± 104	1,281 ± 105

Note. <MDL refers to below the method detection limit, as stated in Table S1.
[a]Averages from the summer of 2015 only include the months of August and September as no sampling occurred in the earlier summer months.

as precipitation. Sharma et al. (2019) found a decrease of Ca^{2+} concentrations of 27% from 1980 to 2013 at Alert in the late summer and early autumn and a small increase of 5% in the summer. Since these inorganic ions would also be present in sea salt, concentrations of nss-K^+, nss-Mg^{2+}, and nss-Ca^{2+} were calculated in order to determine the importance of road dust, crustal material, and biomass burning (Table 1). At Utqiaġvik, nss ions were on average 30% (K^+), 22% (Mg^{2+}), and 40% (Ca^{2+}) of the total compound concentration. At Oliktok Point they were on average 45% (K^+), 32% (Mg^{2+}), and 72% (Ca^{2+}) of the total concentration. Mg^{2+} and Ca^{2+} have been attributed to windblown soil (Barrie & Barrie, 1990). An Arctic dust modeling study found that the contribution of local sources to dust deposition peaked in the autumn while remote sources were more important in the spring (Zwaaftink et al., 2016). Oliktok Point had significantly higher contributions of terrestrial origin than Utqiaġvik when using the paired *t*-test to compare the two sites ($\alpha = 0.05$, $p < 0.005$ [nss-K^+], $p = 0.006$ [nss-Mg^{2+}], $p < 0.005$ [nss-Ca^{2+}]). This is likely due to higher activity surrounding the site leading to more road dust and also because Oliktok Point is more influenced by air masses traveling over land when the two sites are compared using the paired *t*-test ($\alpha = 0.05$, $p < 0.005$).

Organic acids that were detected at the sites varied greatly in concentration (Table 1). MSA has been observed to be predominantly in the fine aerosol fraction (Leck & Persson, 1996; Quinn et al., 2009) and was found to be in the submicron for the 1998–2013 data set used here (see section 2). Based on those results for Utqiaġvik, the TSP measurements here will be considered to be approximately equivalent to long-term $PM_{2.5}$ measurements. Ambient concentrations of MSA were generally higher at Utqiaġvik than Oliktok Point and are significantly different based on the paired *t*-test ($\alpha = 0.05$, $p = 0.048$). Ghahremaninezhad et al. (2019) reported that a global environmental systems model focused on the North American Arctic and Arctic Ocean indicated that the higher concentrations of DMS were expected in the Bering Sea and Bering Strait region than in other regions of the Arctic Ocean. Galí et al. (2019) found that the Bering Sea had some of the higher DMS fluxes along with the Iceland Basin and the Northern Atlantic Ocean. High DMS production has also been observed in the southernmost region of the Chukchi Sea (Park et al., 2019). The advantage to this synoptic study at two coastal NSA sites is the geographic differences in marine air mass influence. Based on the 48-hr back trajectories, during the sample time periods in this study (summers of 2015–2017), Utqiaġvik received marine air masses with 45% from the west, including the Chukchi Sea,

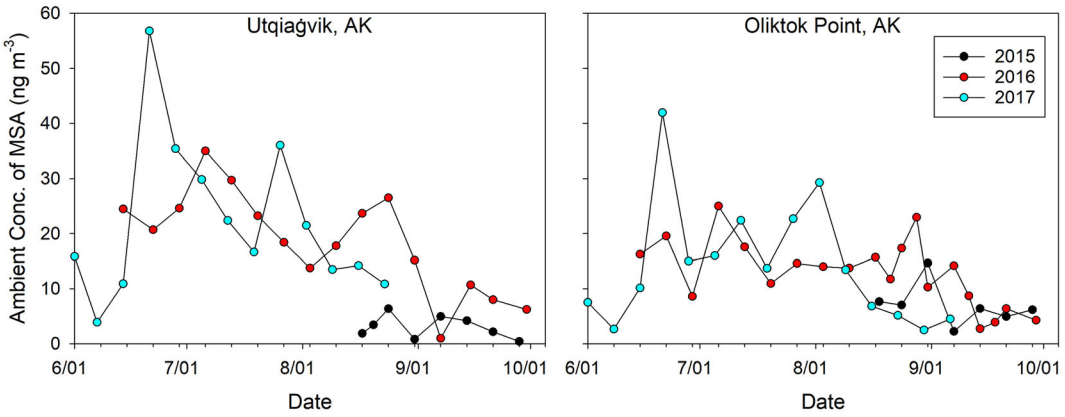

Figure 3. The ambient mass concentration of MSA for the summers of 2015–2017 at each site.

the Bering Strait, and the west coast of Alaska, and 45% from the east, comprised of the Beaufort Sea and the east coast of Alaska (Figure 1). The remaining 10% of air masses traveled over the interior of Alaska. Oliktok Point was also dominated by marine air masses with 67% from the east, only 15% from the west, and 17% from the interior of Alaska. Both sites had less than 1% influence from over Russia. When examining the 1-week back trajectories, source regions of importance remain largely the same, with additional residence time in the Arctic Ocean, the Canadian Arctic Archipelago, and the East Siberian Sea (Figure S2). These different regions may exhibit differences in MSA seasonal trends and responses to local conditions (e.g., temperature, nutrients, and mixing in the water column). Utqiaġvik received more influence from the west which may explain why its concentrations are often higher.

The yearly summer average concentrations ranged from 3.3 ± 0.5 to 22 ± 2 ng m^{-3} at Utqiaġvik and 7 ± 1 to 14 ± 1 ng m^{-3} at Oliktok Point for 2015–2017. At both sites MSA was elevated at the beginning of the summer and decreased into late August and September (Figure 3). This follows previously reported trends of high MSA following the spring blooms of phytoplankton and algae in the Arctic Ocean (Ferek et al., 1995; Leck & Persson, 1996; Park et al., 2017; Quinn et al., 2002). In 2017 the samples collected during the week of 21 June at both sites were statistically high outliers for MSA and nss-SO_4^{2-}. The high MSA and nss-SO_4^{2-} in these two 2017 samples are likely an example of transported marine aerosol impacting the NSA. Seven-day back trajectories for the two sites are very similar, with source regions split between the Beaufort Sea and the Bering Strait (Figure S6). Although the sites were not under continuous cloud cover, satellite images for these two regions have cloud cover which make it difficult to pinpoint the high primary productivity. However, the relationship between MSA and primary productivity measures is not always direct. For example, the summer average from the five source regions do highlight differences in primary productivity by marine regions but do not correlate to MSA concentrations at either site (Figure S7). Variations in chlorophyll-a are not always directly related to primary productivity, and in those instances they would also likely not correlate to MSA or DMS concentrations (Becagli et al., 2016). However, this does not mean that primary productivity in these regions is not responsible for MSA concentrations on the NSA.

There are several sources of nss-SO_4^{2-} in the Arctic, both biogenic and anthropogenic (Ghahremaninezhad et al., 2016; Norman et al., 1999). Average ambient concentrations of nss-SO_4^{2-} increased each summer from 2015 to 2017 at both sites, which is opposite of annual trends which show a long-term decrease (Breider et al., 2017; Quinn et al., 2009). Nss-SO_4^{2-} correlates with MSA at both sites, with an r^2 of 0.49 at Utqiaġvik and 0.50 at Oliktok Point. The correlation indicates a biogenic influence on nss-SO_4^{2-} on the NSA, which aligns with previous studies which reported a significant contribution of marine sources to sulfate aerosol in the summertime Arctic (Breider et al., 2017; Li & Barrie, 1993; Park et al., 2017). Similarly, sulfur isotope data revealed between 9% and 40% of nss-SO_4^{2-} were from biogenic sources in the Canadian Arctic summer in the early 1990s, and up to 70% of nss-SO_4^{2-} resulted from DMS in the early summer in Svalbard in 2015 (Norman et al., 1999; Park et al., 2017). Studies have also shown that the contribution of biogenic sulfate to the total sulfate increases with increasing MSA concentrations (Park et al., 2017).

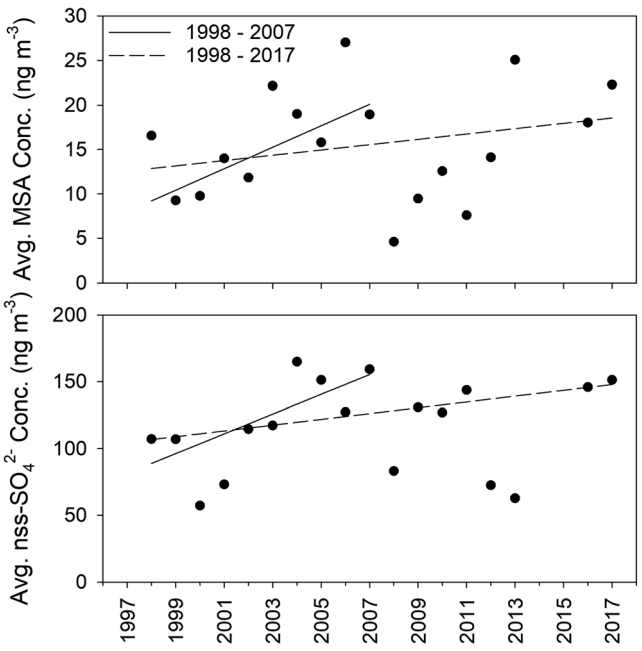

Figure 4. Average MSA (top) and nss-SO_4^{2-}(bottom) mass concentrations for July–September over two decades. The lines represent the Sen's slope estimates. The 1998–2017 line does not include the summer of 2015.

However, anthropogenic contributions are also likely for nss SO_4^{2-} at both NSA sites, and the correlation analysis does not fully reflect the complexity of the atmospheric chemistry and transport influences on the ratio of MSA:nss-SO_4^{2-}. At Oliktok Point anthropogenic influences would include local oil and gas exploration and extraction activity and potential long-range transport. Indeed, ATOFMS measurements showed primary sulfate mixed with local combustion soot at the site (Gunsch et al., 2019). At Utqiaġvik anthropogenic nss-SO_4^{2-} is likely due to transport from source regions including oil field activity surrounding Oliktok Point; Gunsch et al. (2017) observed days with influence from the NSA oil fields during September 2015. It is also possible that the measured MSA represents a lower limit of the MSA produced in source regions due to loss from oxidation during atmospheric transport to the site (Mungall et al., 2018). It is important to consider both MSA and nss-SO_4^{2-} to understand Arctic atmospheric composition.

3.2. Long-Term Trends of MSA and Nss-SO_4^{2-}

Quinn et al. (2009) reported MSA and nss-SO_4^{2-} for filter samples from Utqiaġvik, AK, from 1998 to 2007, and demonstrated an increase in summertime MSA and nss-SO_4^{2-} ambient concentrations over that decade. They reference decreasing sea ice cover and increases in mean sea surface temperature as potential causes of these trends (Quinn et al., 2009). By combining the published measurements, additional MSA and nss-SO_4^{2-} for 2008–2013 from NOAA, and the 2016–2017 ARM field campaign results, trends over two decades on the NSA can be evaluated. The Mann-Kendall test and Sen's method were used to test for monotonic trends and estimate the slope of the linear trend. Quinn et al. (2009) defined summer months as July–September; those months were used to calculate the averages used for this comparison. The summer of 2015 is excluded here as it does not include July, which is an important month for primary productivity; the August–September 2015 MSA average is significantly lower than the other two years in this study (Table S3). Comparing the summer averages for the full summer (Table 1) to the averages for just August–September (Table S3), the effects of July primary productivity on nss-SO_4^{2-} are evident; 2015 was also excluded from the trend for nss-SO_4^{2-} for this reason. The average nss-SO_4^{2-} concentration in 2015 is significantly different from the summers of 2016 ($\alpha = 0.05$, $p = 0.01$) and 2017 ($\alpha = 0.05$, $p = 0.04$) when considering the full summer. The summer of 2017 average concentration decreases when only examining the months of August–September and is similar to that of the summer of 2015. The average concentration of nss-SO_4^{2-} for 2016 increases when the earlier summer months are excluded, highlighting the influence of the Extreme Arctic Cyclone of 2016 on primary productivity, discussed in section 3.4.

Quinn et al. (2009) reported an increase of MSA concentrations of 12% per year ($\alpha = 0.1$) from 1998 to 2007. With the addition of 2008–2013, 2016, and 2017, the increase of MSA concentrations is 2.5 ± 4.0% per year ($\alpha > 0.10$) (Figure 4). Quinn et al. (2009) found an increase of 8% per year ($\alpha = 0.05$) in nss-SO_4^{2-} concentration. With the addition of the data from this study, the trend is still increasing but at a rate of 2.1 ± 14% per year ($\alpha > 0.10$). There is an apparent decrease in the magnitude of both upward trends with the additional summers of data. Environmental and climate factors may be contributing to the reduced rate of increase in MSA and nss-SO_4^{2-} concentrations in Utqiaġvik. DMS emissions in the open water regions of the Arctic Ocean increased rapidly from 2003 to 2011 and then decreased from 2011 to 2016 (Galí et al., 2019). The data from Quinn et al. (2009) reflect this in the MSA concentrations, while the additional data in this study show the result of decreased DMS emissions. In addition, sea ice extent has retreated significantly over this time, such that the primary production zones on the ice edge are less influential on aerosol at Utqiaġvik during the summer. Previous studies have also hypothesized that in July–August the ice edge has receded enough that it no longer effects areas of high productivity (Sharma et al., 2012). Indeed, monthly average ice extent reveals that the sea ice extent reduces drastically in the region in 2007 and remains similarly diminished during the next decade (Figure S8). In the summer of 2013, the sea ice extent is more similar to years prior to 2007 and also has a higher average concentration of MSA (Figures 4 and S8). A linear regression of monthly average

sea ice extent with MSA for 1998–2017 reveals a weak correlation with $r^2 = 0.17$ (Figure S9). The upward trend of the data indicates a minor influence of sea ice extent, most likely due to proximity of the sea ice edge to the NSA. As the ice edge retreats further from the NSA coast, MSA produced from these zones of high primary productivity may be diluted during transport to the NSA sites. This analysis indicates conflicting processes that need to continue to be monitored: enhanced primary productivity associated with temperature resulting in higher biogenic sulfur aerosols versus dilution of the measured MSA as productive regions on the ice edge move further from the NSA coast.

Sharma et al. (2019) found no significant change in MSA concentrations between 1980 and 2013 at Alert. An increase of 4% per year in MSA was reported at Alert between 1998 and 2008 (Sharma et al., 2012). Similar to Quinn et al. (2009), the increase over the time period was attributed potentially to reduced sea ice (Sharma et al., 2012). Sharma et al. (2019) concluded that high MSA concentrations before 1990 were not related to sea ice reduction. Ice extent has been affected more intensely in the Beaufort and Chukchi Seas than in the regions surrounding Alert (Comiso, 2012). The effects of increased primary productivity due to changes in sea ice extent might be more readily observed in regions like the NSA. On a longer time scale, MSA concentrations from the Greenland ice sheet started to decline in 1816 at the onset of regional warming associated with the industrial revolution (Osman et al., 2019). This decrease is thought to be associated with a reduction in North Atlantic primary productivity caused by a weakened Atlantic meridional overturning circulation (Osman et al., 2019). Clearly, ongoing measurements are needed to determine short- and long-term responses to climate change at different Arctic sites.

In terms of atmospheric chemistry, there is a temperature dependency of DMS oxidation to MSA versus sulfate, with sulfate favored at higher temperatures (Albu et al., 2006; Jung et al., 2014). Bates et al. (1992) calculated that decreasing the temperature from 25°C to 5°C results in an increase of a factor of 3.8 in the production of MSA over nss-SO_4^{2-}. The formation of MSA is favored at temperatures under 17°C (Jung et al., 2014). It is possible that air temperatures have warmed in source regions so that the formation of sulfate is then favored over MSA. Examining the ambient temperature data reported by the HYSPLIT program with the back trajectories, some back trajectories did have maximum temperatures associated with them greater than 17°C. These high temperatures mainly occurred over land, either the interior of Alaska or Russia, or along the coasts of Alaska and the Bering Strait. Overall, however, the average temperatures were never above 17°C. Because these data are reported by the HYSPLIT model, they may not be fully representative of the meteorological conditions in each source region. Understanding trends in nss-SO_4^{2-} is difficult due to the multiple sources it can have. Annual anthropogenic emissions of sulfate have decreased over the last decades (Breider et al., 2017; Hirdman et al., 2010; Quinn et al., 2009; Sharma et al., 2006), although this is not necessarily true for local emissions from Prudhoe Bay. It is possible that nss-SO_4^{2-} from marine biogenic emissions has increased, but quantifying that contribution to the total nss-SO_4^{2-} is outside the scope of this study.

The increasing concentrations of marine sulfur aerosols may have implications for cloud-aerosol interactions in the future. The κ of sulfate is higher than that of methanesulfonate compounds; however, any size distribution changes likely will dominate any potential differences in CCN activity. MSA:nss-SO_4^{2-} mass concentration ratios ranged from 0.30% to 52% between 1997 and 2017, with an average ratio of 16 $\pm$ 14%. These values are similar to previously reported values of below 0.2% and up to 32% in campaigns over the Southern Pacific Ocean and the Canadian Arctic Archipelago (Bates et al., 1992; Willis et al., 2017). Leck and Persson (1996) found a constant MSA:nss-SO_4^{2-} molar ratio of 22% during the summer and autumn of 1991 over the Arctic Ocean and pack ice. Sharma et al. (2019) found an average molar MSA:nss-SO_4^{2-} ratio of 13.5 $\pm$ 6% at Alert. These ratios likely incorporate both differences due to the contributions of sources (e.g., marine and anthropogenic) and differences associated with temperature controls on MSA production in the atmosphere. Understanding influences on MSA and nss-SO_4^{2-}, such as temperature, is important as the climate continues to change and influence aerosol, with potential feedbacks through cloud-aerosol interactions. Composition, mixing state, and CCN measurements are all relevant to improve predictions of the effects of increased marine biogenic aerosol on cloud-aerosol interactions in the Arctic.

3.3. Relationship Between Temperature and MSA

Previous research using ice cores has indicated that MSA concentrations are related to warmer sea surface temperature and reduced sea ice extent, which is cited by Quinn et al. (2009) as a potential

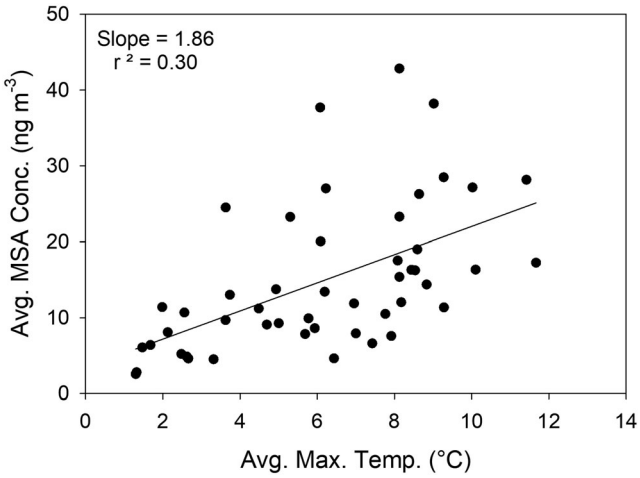

Figure 5. The average monthly concentration of MSA plotted against the average monthly maximum temperature at Utqiaġvik (1998–2017).

influence on increasing MSA concentrations (O'Dwyer et al., 2000). As mentioned above, the longer record in the Greenland ice sheet indicates a long-term decreasing trend with the last 20 years increasing (Osman et al., 2019; Sharma et al., 2019). The potential relationship is complex and can be examined on different time scales (Osman et al., 2019). The monthly averages of MSA from 1998–2013 and 2015–2017 were plotted versus the average maximum temperature at Utqiaġvik and show a weak relationship with an $r^2 = 0.30$ (Figure 5). The average maximum temperature was selected to capture the relationship of the higher daily temperatures with MSA, which the average temperature may not properly show.

Warmer months likely have increased primary productivity leading to higher concentrations of MSA. In addition, air masses may be passing over warmer marine regions with increased biogenic activity, bringing both higher temperatures and marine aerosol. No relationship ($r^2 < 0.10$) was found for average maximum temperature and nss-SO_4^{2-}, potentially due to the influence of multiple sources. Previous research found a strong inverse relationship between MSA:nss-SO_4^{2-} and atmospheric temperature (Bates et al., 1992). This study found a weaker positive relationship ($r^2 = 0.15$, slope = 1.37) with the ratio of MSA:nss-SO_4^{2-} than with MSA alone. The differing relationships are likely due to differences in the sampling sites including marine biogenic source regions and temperature; the average daily temperature in Bates et al. (1992) was as high as 28°C, while the largest average maximum temperature for this study was 12°C. With sulfate production from DMS favored as temperatures increase, it is possible that an inverse relationship may be observed on the NSA in the future as temperatures rise. However, because nss-SO_4^{2-} also has anthropogenic sources on the NSA which may not change with temperature, this relationship may be difficult to assess.

In order to study the short-term connection among nss-SO_4^{2-}, MSA, and temperature, the same correlation was performed with the individual data points from 2015 to 2017. As there may be a delay in the effect of warmer temperatures on DMS production, the weeklong duration of the samples may help appropriately capture this relationship. The high concentration samples from 2017 are excluded in these relationships as they were determined to be statistical outliers. Nss-SO_4^{2-} was weakly correlated with temperature at both Utqiaġvik ($r^2 = 0.27$, slope = 8.55) and Oliktok ($r^2 = 0.22$, slope = 6.46) between 2015 and 2017. As mentioned before, it may be difficult to identify connections between nss-SO_4^{2-} as it has multiple sources ranging from biogenic to anthropogenic. There is a stronger relationship between weekly MSA and the corresponding weekly average maximum temperature ($r^2 = 0.41$, slope = 1.26) (Figure 6), although there are key differences between the sites. All three summers at Oliktok Point (2015–2017) have a consistent relationship between MSA and temperature ($r^2 = 0.62$, slope = 1.10). During the summer of 2015 at Utqiaġvik, there is no relationship ($r^2 < 0.10$) between MSA and temperature. The summer of 2017 at Utqiaġvik has a correlation of $r^2 = 0.45$. The summer of 2016 at Utqiaġvik has a strong relationship with temperature ($r^2 = 0.84$, slope = 2.83). While Oliktok Point always has a large portion of its air mass influence from the Beaufort Sea each summer, Utqiaġvik has varying influence (Figure S10). A previous study in the Arctic Ocean found that changes in transport patterns between days, seasons, and years had large effects on the atmospheric sulfur budget (Nilsson & Leck, 2002). The consistent Beaufort Sea influence and correlation between temperature and MSA at Oliktok Point indicate that year-to-year differences in concentration are likely due to changes to the environment and not shifting air mass source regions. Previous studies have found differing relationships between temperature and MSA, with studies in subpolar regions finding weak relationships (Bates et al., 1992; Jung et al., 2014). A study in the open Arctic Ocean reported no temperature dependence (Leck & Persson, 1996), while another at Alert found no direct links between MSA and changes in air temperature (Sharma et al., 2012). Sites with multiple source regions such as Utqiaġvik may make this relationship difficult to study. Oliktok Point is better positioned to understand how variations in sea ice extent from year to year affect primary productivity. The Arctic Ocean is comprised of multiple biogeochemical regimes which will all react differently to changing temperatures and sea ice extent (Galí et al., 2019). An understanding of how each region is affected is necessary to comprehend how emissions of MSA and

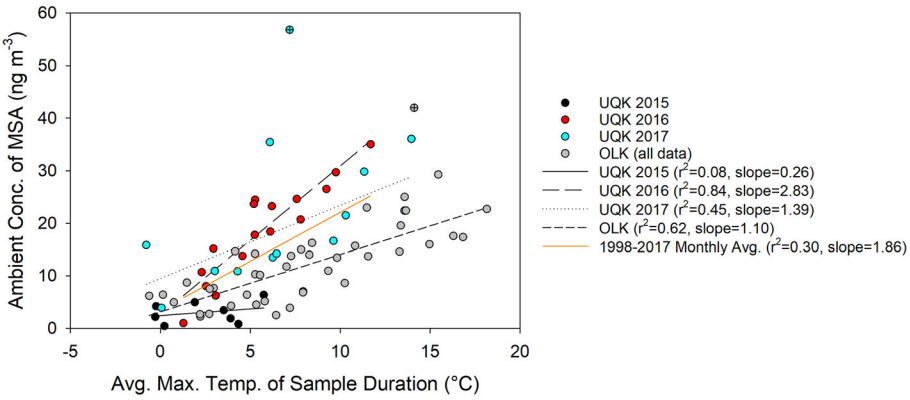

Figure 6. A scatter plot of the ambient concentration of MSA for both Utqiaġvik and Oliktok Point and the average maximum temperature of the sample duration. Utqiaġvik has individual trendlines for each summer while Oliktok Point is represented by a single trendline as the relationship is consistent over all three summers (2015–2017). The trendline for the monthly averages from 1998 to 2017 is also included. The two statistical outliers are marked with a +.

aerosol-cloud interactions may change. Continued long-term sampling at Arctic sites like Oliktok Point would allow for this understanding of the Beaufort Sea.

3.4. Influence of Arctic Cyclones on MSA

The Extreme Arctic Cyclone of August 2016 may have affected the air mass influence on Utqiaġvik as the average back trajectory contribution for the summer of 2016 had a higher percent contribution from the Chukchi Sea than all other summers. In addition, the cyclone may have led to increased primary productivity in regions of the Arctic Ocean that influenced Utqiaġvik. Simmonds and Rudeva (2014) reported cyclones in July 2002 and 2003, as well as September 2003. The cyclones in July were the first and third ranked cyclones that occurred in July between 1979 and 2009 (Simmonds & Rudeva, 2014). Like the summer of 2016, the summers of 2002 and 2003 also show strong relationships between MSA concentration and the average maximum temperature (Figure 7). The summer of 2012, when the Great Arctic Cyclone of August 2012 occurred, does not show this strong relationship, although primary productivity was shown to increase due to enhanced nutrients associated with vertical mixing (Zhang et al., 2014). As this cyclone occurred in a time of decreased DMS emissions (Galí et al., 2019), it potentially only increased what was already an unproductive year. A study on the impact of Arctic cyclones on chlorophyll-a concentrations found that the increase in concentration was dependent on the initial chlorophyll-a concentrations (Li et al., 2019). The summers of 2002, 2003, and 2016 likely show the result of enhanced productivity due to both warmer temperatures and cyclonic activity. Two other years with strong relationships were 2004 ($r^2 = 0.73$, slope = 2.72) and 2009 ($r^2 = 0.64$, slope = 1.32). No record of an intense cyclone during either summer was found, but that does not rule out similar mixing events. Primary productivity in the Arctic is affected by many factors including temperature, sea ice extent, and nutrient availability. In these years with intense cyclonic activity, ambient maximum temperature is a strong indicator of MSA concentrations. The exact mechanisms behind this relationship, including effects on air mass influence and increased nutrients for phytoplankton blooms, need to be studied more in depth. The remaining summers either had strong relationships with few data points or had relationships more similar to the summers of 2015 and 2017 at Utqiaġvik. The varying source regions as well as the potential impacts of long-range transport of MSA and other aerosol make identifying a relationship between MSA and temperature difficult for these summers. Transported MSA may relate differently to temperature or other parameters than MSA formed near the site.

3.5. Mixing State of MSA

The mixing state of MSA within the aerosol population, or distribution of MSA across individual particles, was determined by real-time measurements of individual aerosol particles by ATOFMS at Oliktok Point. This analysis facilitates understanding of sources of the submicron MSA-containing particles, which provides improved understanding of potential CCN impacts. For 22 August to 17 September 2016, MSA (m/z −95 [$CH_3SO_3^-$]) was observed within 3%, by number of the 32,880 measured, of 0.07–1.6 μm (vacuum aerodynamic diameter) particles, varying from 0% to 17% of the number concentration over the

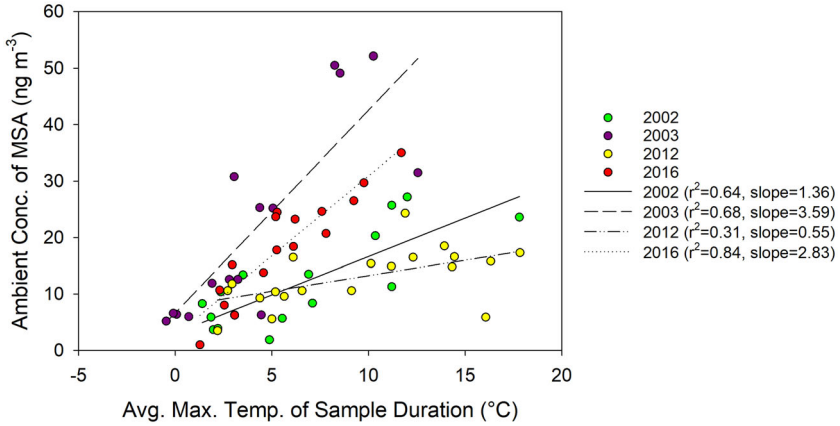

Figure 7. A scatter plot of the ambient concentration of MSA versus the average maximum temperature of the sample duration for the four summers at Utqiaġvik with recorded Arctic cyclones.

course of the study. Ninety-seven percent of the MSA-containing particles, by number, were classified as OC-amine-sulfate particles (60%), aged soot (ECOC) particles (25%), and aged sea spray aerosols (12%), with each of these particle types containing additional secondary aerosol components. Compared to the full population of observed OC-amine-sulfate and ECOC particles (Gunsch et al., 2019), the MSA-containing particles had elevated sulfate (m/z −97 [HSO_4^-]) and oxidized organics (m/z +43 [$C_2H_3O^+$]) (Qin et al., 2012) signals (Figure 8). MSA was detected in chloride-depleted sea spray particles (lack of m/z −93 [$NaCl_2^-$] or −97 [$NaCl_2^-$] peaks), which is consistent with atmospheric aging due to reactions with acids resulting in HCl release. Due to potential interferences, MSA could not be accurately measured in particles

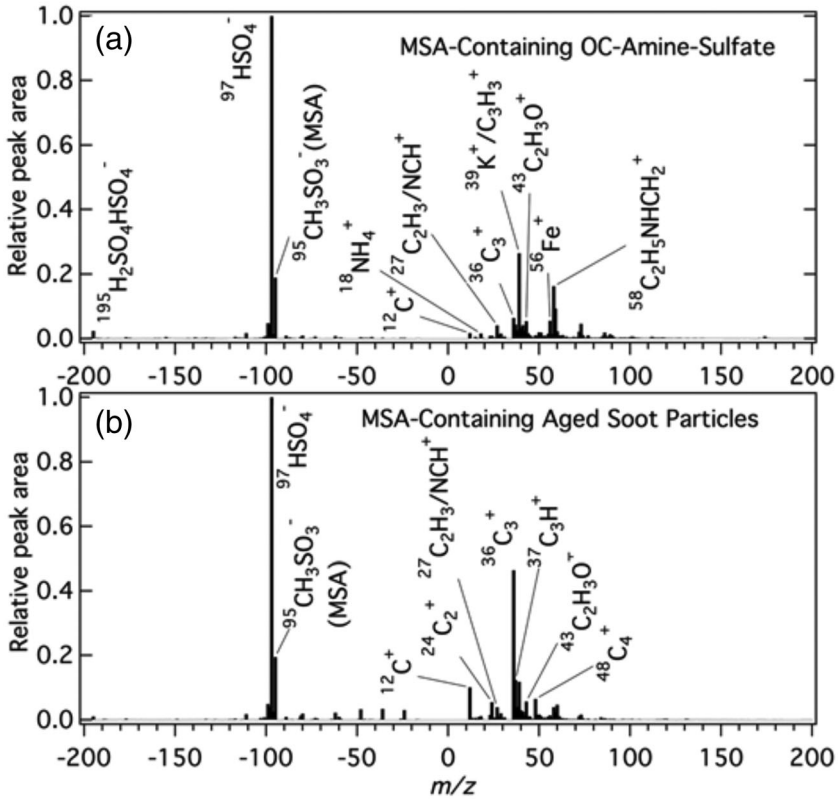

Figure 8. Average individual particle ATOFMS mass spectra for MSA-containing (a) OC-amine-sulfate and (b) aged soot particles.

with m/z −93 ($NaCl_2^-$) or −97 ($NaCl_2^-$) peaks. MSA was previously found to be internally mixed within aged soot and sea spray aerosols at Riverside, California, located approximately 100 km from the coast (Gaston et al., 2010), and in organic and amine-containing particles at a remote Arctic area of Resolute Bay, Nunavut, Canada (Köllner et al., 2017; Willis et al., 2017). In this study, 85%, 72%, and 45% of MSA-containing particles, by number, were internally mixed with sulfate, oxidized organics, and ammonium (m/z +18 [NH_4^+]), respectively, consistent with significant accumulation of secondary aerosol. OC-amine-sulfate and soot particles were emitted within the oil field (Gunsch et al., 2019), suggesting condensation of MSA and other secondary species during transport across the oil field. Iron (m/z + 54, 56, 57 [Fe^+]) was internally mixed in 44%, by number, of MSA-containing OC-amine-sulfate particles, and the Fe peaks were significantly higher in these particles compared to the rest of OC-amine-sulfate particles. Iron could act as a catalyst for MSA formation (Alexander et al., 2009), as suggested previously for vanadium observed within MSA-containing particles in California by Gaston et al. (2010). These results indicate that MSA condenses onto preexisting particles within the oil fields and accumulates with significant secondary sulfate and organics, highlighting the importance of marine emissions even in regions with oil and gas emissions.

4. Conclusions

This study presents trends in MSA and nss-SO_4^{2-} concentration over several years and examines how the changing Arctic influences the aerosol concentration and composition. Both sites (Utqiaġvik and Oliktok Point, AK) had similar concentrations of MSA, despite having differing influence from air mass source regions. When combined with additional data sets at Utqiaġvik, MSA and nss-SO_4^{2-} concentrations have increased over the last two decades at a rate of +2.5% per year and + 2.1% per year, respectively. MSA: nss-SO_4^{2-} ratios indicate that nss-SO_4^{2-} has both biogenic and anthropogenic sources. The average ratio of MSA to nss-SO_4^{2-} is similar to those reported in other polar regions. Biogenic sulfur compounds could potentially influence cloud-aerosol interactions as the climate changes in the Arctic. At Oliktok Point, MSA was observed within individual OC-amine-sulfate and aged soot particles with significant secondary sulfate and oxidized organics, highlighting the importance of marine aerosol in an oil field. The relationship between MSA and OC could provide information about the factors driving OC composition.

Monthly averages of MSA from 1997 to 2017 are weakly related to ambient temperature, suggesting that warmer temperatures explain some increases in marine biogenic activity and aerosol. MSA concentrations have a strong relationship to ambient temperature at Oliktok Point, where air mass influence is predominantly from the Beaufort Sea. Utqiaġvik, where MSA is weakly related to ambient temperature, receives air mass influence from multiple marine and coastal regions making it more difficult to observe these relationships. Warmer temperatures will affect primary productivity differently in each region. Nss-SO_4^{2-} is weakly related to temperature from 2015 to 2017 at each site but has no relationship over 1997–2017, likely due to multiple sources aside from marine influencing its concentrations. Summers with intense Arctic cyclone activity at Utqiaġvik had strong relationships between MSA and average maximum temperature, perhaps due to enhanced vertical mixing in the surface ocean. More research is needed to determine how the complex Arctic marine system including ocean circulation, cyclonic activity, and changes in plankton populations impacts DMS emission and MSA and nss-SO_4^{2-} production.

Data Availability Statement

The ion chromatography data used in this paper can be accessed online (at https://dataverse.tdl.org/dataverse/baylor using http://10.18738/T8/EVQCQB). The ATOFMS data can be accessed through the ARM Data Center (Pratt, 2016). Meteorological and aerosol data for Utqiaġvik were obtained from NOAA Earth System Research Laboratory Global Monitoring Laboratory (https://www.esrl.noaa.gov/gmd/obop/brw/). Meteorological data for Oliktok Point were obtained from the Atmospheric Radiation Measurement (ARM) Program sponsored by the U.S. Department of Energy, Office of Science, Office of Biological and Environmental Research, Climate and Environmental Sciences Division (Kyrouac & Holdridge, 2015) (https://doi.org/10.5439/1025220). Chlorophyll data are provided by the NASA Ocean Biology Processing group and can be accessed online (using https://doi.org/10.5067/NPP/VIIRS/L3B/CHL/2018). Sea ice extent data are provided by the National Snow and Ice Data Center and is accessible online (using https://doi.org/10.7265/N5K072F8).

Acknowledgments

The authors gratefully acknowledge the NOAA Air Resources Laboratory (ARL) for the provision of the HYSPLIT transport and dispersion model and/or READY website (http://www.ready.noaa.gov) used in this publication. The authors would also like to thank the National Aeronautics and Space Administration Ocean Biology Processing Group (OBPG) for providing the Suomi NPP Chlorophyll Data. Financial and technical support for this campaign was provided by the United States Department of Energy (ARM Field Campaign nos 2013-6660 and 2014-6694 and Early Career Award no. DE-SC0019172), NOAA (award nos NA14OAR4310150 and NA14OAR4310149), the C. Gus Glasscock, Jr. Endowed Fund for Excellence in Environmental Sciences, and the Baylor University BTRUE program. The authors would like to thank the Baylor University Center for Reservoir and Aquatic Systems Research for access to the instrumentation for ion chromatography analysis. They would also like to thank the United States Air Force and Sandia National Laboratory, including Fred Helsel, Dan Lucero, and Jeffrey Zirzow, for site access and preparation, and Wessley King, Joshua Remitz, Ben Bishop, and David Oaks, and the Ukpeaġvik Iñupiat Corporation, specifically Walter Brower and Jimmy Ivanoff for sample collection and field assistance. The authors would like to thank Tom Watson for assisting in processing satellite data. This is PMEL contribution number 5073 and JISAO contribution 2020-1111.

References

Abbatt, J. P., Leaitch, W. R., Aliabadi, A. A., Bertram, A. K., Blanchet, J.-P., Boivin-Rioux, A., et al. (2019). Overview paper: New insights into aerosol and climate in the Arctic. *Atmospheric Chemistry and Physics*, *19*(4), 2527–2560.

Albu, M., Barnes, I., Becker, K. H., Patroescu-Klotz, I., Mocanu, R., & Benter, T. (2006). Rate coefficients for the gas-phase reaction of OH radicals with dimethyl sulfide: Temperature and O_2 partial pressure dependence. *Physical Chemistry Chemical Physics*, *8*(6), 728–736. https://doi.org/10.1039/b512536g

Alexander, B., Park, R. J., Jacob, D. J., & Gong, S. (2009). Transition metal-catalyzed oxidation of atmospheric sulfur: Global implications for the sulfur budget. *Journal of Geophysical Research*, *114*, D02309. https://doi.org/10.1029/2008JD010486

Barrett, T., Robinson, E., Usenko, S., & Sheesley, R. (2015). Source contributions to wintertime elemental and organic carbon in the western arctic based on radiocarbon and tracer apportionment. *Environmental Science & Technology*, *49*(19), 11,631–11,639. https://doi.org/10.1021/acs.est.5b03081

Barrett, T. E., & Sheesley, R. J. (2014). Urban impacts on regional carbonaceous aerosols: Case study in central Texas. *Journal of the Air & Waste Management Association*, *64*(8), 917–926. https://doi.org/10.1080/10962247.2014.904252

Barrie, L., & Barrie, M. (1990). Chemical components of lower tropospheric aerosols in the high Arctic: Six years of observations. *Journal of Atmospheric Chemistry*, *11*(3), 211–226.

Bates, T. S., Calhoun, J. A., & Quinn, P. K. (1992). Variations in the methanesulfonate to sulfate molar ratio in submicrometer marine aerosol particles over the South Pacific Ocean. *Journal of Geophysical Research*, *97*(D9), 9859–9865. https://doi.org/10.1029/92JD00411

Becagli, S., Amore, A., Caiazzo, L., Iorio, T. D., Sarra, A. D., Lazzara, L., et al. (2019). Biogenic aerosol in the Arctic from eight years of MSA data from Ny Ålesund (Svalbard Islands) and Thule (Greenland). *Atmosphere*, *10*(7), 349. https://doi.org/10.3390/atmos10070349

Becagli, S., Lazzara, L., Marchese, C., Dayan, U., Ascanius, S. E., Cacciani, M., et al. (2016). Relationships linking primary production, sea ice melting, and biogenic aerosol in the Arctic. *Atmosphereic Environment*, *136*, 1–15. https://doi.org/10.1016/j.atmosenv.2016.04.002

Bélanger, S., Babin, M., & Tremblay, J.-É. (2013). Increasing cloudiness in Arctic damps the increase in phytoplankton primary production due to sea ice receding. *Biogeosciences*, *10*(6), 4087–4101. https://doi.org/10.5194/bg-10-4087-2013

Breider, T. J., Mickley, L. J., Jacob, D. J., Ge, C., Wang, J., Sulprizio, M. P., et al. (2017). Multidecadal trends in aerosol radiative forcing over the Arctic: Contribution of changes in anthropogenic aerosol to Arctic warming since 1980. *Journal of Geophysical Research: Atmospheres*, *122*, 3573–3594. https://doi.org/10.1002/2016JD025321

Browse, J., Carslaw, K., Mann, G., Birch, C., Arnold, S., & Leck, C. (2014). The complex response of Arctic aerosol to sea-ice retreat. *Atmospheric Chemistry and Physics*, *14*(14), 7543–7557. https://doi.org/10.5194/acp-14-7543-2014

Chen, Y., & Bond, T. (2010). Light absorption by organic carbon from wood combustion. *Atmospheric Chemistry and Physics*, *10*(4), 1773–1787.

Christison, T., Saini, C., & Lopez, L. (2015). *Application note: Determination of organic acids in beer samples using a high-pressure ion chromatography system*. Sunnyvale, CA, USA: Thermo Fisher Scientific.

Clegg, S. L., Brimblecombe, P., & Wexler, A. S. (1998). Thermodynamic model of the system H^+–NH_4^+–SO_4^{2-}–NO_3^-–H_2O at tropospheric temperatures. *The Journal of Physical Chemistry A*, *102*(12), 2137–2154. https://doi.org/10.1021/jp973042r

Comiso, J. C. (2012). Large decadal decline of the Arctic multiyear ice cover. *Journal of Climate*, *25*(4), 1176–1193. https://doi.org/10.1175/JCLI-D-11-00113.1

Croft, B., Martin, R. V., Leaitch, W. R., Tunved, P., Breider, T. J., D'Andrea, S. D., & Pierce, J. R. (2016). Processes controlling the annual cycle of Arctic aerosol number and size distributions. *Atmospheric Chemistry and Physics*, *16*(6), 3665–3682. https://doi.org/10.5194/acp-16-3665-2016

Di Pierro, M., Jaeglé, L., Eloranta, E., & Sharma, S. (2013). Spatial and seasonal distribution of Arctic aerosols observed by CALIOP (2006–2012). *Atmospheric Chemistry and Physics Discussions*, *13*(2), 4863–4915. https://doi.org/10.5194/acpd-13-4863-2013

Dickson, A. G., & Goyet, C. (1994). *Handbook of methods for the analysis of the various parameters of the carbon dioxide system in sea water. Version 2*. United States. https://doi.org/10.2172/10107773

Dusek, U., Frank, G., Hildebrandt, L., Curtius, J., Schneider, J., Walter, S., et al. (2006). Size matters more than chemistry for cloud-nucleating ability of aerosol particles. *Science*, *312*(5778), 1375–1378. https://doi.org/10.1126/science.1125261

Ferek, R. J., Hobbs, P. V., Radke, L. F., Herring, J. A., Sturges, W. T., & Cota, G. F. (1995). Dimethyl sulfide in the arctic atmosphere. *Journal of Geophysical Research*, *100*(D12), 26,093–26,104. https://doi.org/10.1029/95JD02374

Fetterer, F., Knowles, K., Meier, W. N., Savoie, M., & Windnagel, A. K. (2017). *Updated daily. Sea ice index, version 3. Jul.–Sept. 1998–2017*. Boulder, Colorado, USA: NSIDC: National Snow and Ice Data Center. https://doi.org/10.7265/N5K072F8 Data set accessed 2020-07-26

Galí, M., Devred, E., Babin, M., & Levasseur, M. (2019). Decadal increase in Arctic dimethylsulfide emission. *Proceedings of the National Academy of Sciences*, *116*(39), 19,311–19,317. https://doi.org/10.1073/pnas.1904378116

Gaston, C. J., Pratt, K. A., Qin, X., & Prather, K. A. (2010). Real-time detection and mixing state of methanesulfonate in single particles at an inland urban location during a phytoplankton bloom. *Environmental Science & Technology*, *44*(5), 1566–1572. https://doi.org/10.1021/es902069d

Ghahremaninezhad, R., Gong, W., Galí, M., Norman, A.-L., Beagley, S. R., Akingunola, A., et al. (2019). Dimethyl sulfide and its role in aerosol formation and growth in the Arctic summer—A modelling study. *Atmospheric Chemistry and Physics*, *19*(23), 14,455–14,476. https://doi.org/10.5194/acp-19-14455-2019

Ghahremaninezhad, R., Norman, A.-L., Abbatt, J. P., Levasseur, M., & Thomas, J. L. (2016). Biogenic, anthropogenic, and sea salt sulfate size-segregated aerosols in the Arctic summer. *Atmospheric Chemistry and Physics*, *16*, 5191–5202. https://doi.org/10.5194/acp-16-5191-2016

Giardi, F., Becagli, S., Traversi, R., Frosini, D., Severi, M., Caiazzo, L., et al. (2016). Size distribution and ion composition of aerosol collected at Ny-Ålesund in the spring–summer field campaign 2013. *Rendiconti Lincei*, *27*(1), 47–58. https://doi.org/10.1007/s12210-016-0529-3

Gilbert, R. O. (1987). *Statistical methods for environmental pollution monitoring*. New York, NY: John Wiley & Sons.

Gourdal, M., Lizotte, M., Massé, G., Gosselin, M., Poulin, M., Scarratt, M., et al. (2018). Dimethyl sulfide dynamics in first-year sea ice melt ponds in the Canadian Arctic Archipelago. *Biogeosciences*, *15*(10), 3169–3188. https://doi.org/10.5194/bg-15-3169-2018

Gunsch, M. J., Kirpes, R. M., Kolesar, K. R., Barrett, T. E., China, S., Sheesley, R. J., et al. (2017). Contributions of transported Prudhoe Bay oil field emissions to the aerosol population in Utqiagvik, Alaska. *Atmospheric Chemistry and Physics (Online)*, *17*. https://doi.org/10.5194/acp-17-10879-2017

Gunsch, M. J., Liu, J., Moffett, C. E., Sheesley, R. J., Wang, N., Zhang, Q., et al. (2019). Diesel soot and amine-containing organic sulfate aerosols in an Arctic oil field. *Environmental Science & Technology*, *54*(1), 92–101. https://doi.org/10.1021/acs.est.9b04825

Hatakeyama, S., Izumi, K., & Akimoto, H. (1985). Yield of SO_2 and formation of aerosol in the photo-oxidation of DMS under atmospheric conditions. *Atmospheric Environment (1967)*, *19*(1), 135–141. https://doi.org/10.1016/0004-6981(85)90144-1

Heintzenberg, J., Tunved, P., Galí, M., & Leck, C. (2017). New particle formation in the Svalbard region 2006–2015. *Atmospheric Chemistry and Physics*, *17*(10). https://doi.org/10.5194/acp-17-6153-2017

Hirdman, D. A., Burkhart, J. F., Sodemann, H., Eckhardt, S., Jefferson, A., Quinn, P. K., et al. (2010). Long-term trends of black carbon and sulphate aerosol in the Arctic: Changes in atmospheric transport and source region emissions. *Atmospheric Chemistry and Physics*, *10*, 9351–9368. https://doi.org/10.5194/acp-10-9351-2010

Holland, H. D. (1978). *The chemistry of the atmosphere and oceans-(v.1)*. New York, NY: Wiley-Interscience.

Jung, J., Furutani, H., Uematsu, M., & Park, J. (2014). Distributions of atmospheric non-sea-salt sulfate and methanesulfonic acid over the Pacific Ocean between 48°N and 55°S during summer. *Atmospheric Environment*, *99*, 374–384. https://doi.org/10.1016/j.atmosenv.2014.10.009

Kahru, M., Brotas, V., Manzano-Sarabia, M., & Mitchell, B. (2011). Are phytoplankton blooms occurring earlier in the Arctic? *Global Change Biology*, *17*(4), 1733–1739. https://doi.org/10.1111/j.1365-2486.2010.02312.x

Kahru, M., Lee, Z., Mitchell, B. G., & Nevison, C. D. (2016). Effects of sea ice cover on satellite-detected primary production in the Arctic Ocean. *Biology Letters*, *12*(11), 20,160,223. https://doi.org/10.1098/rsbl.2016.0223

Köllner, F., Schneider, J., Willis, M. D., Klimach, T., Helleis, F., Bozem, H., et al. (2017). Particulate trimethylamine in the summertime Canadian high Arctic lower troposphere. *Atmospheric Chemistry and Physics*, *17*(22), 13,747–13,766. https://doi.org/10.5194/acp-17-13747-2017

Kyrouac, J., & Holdridge, D. (2015). *Updated hourly. Surface meteorological instrumentation (MET). Aug. 2015–Oct. 2015, Jun. 2016–Oct. 2016, Jun. 2017–Oct. 2017. ARM Mobile Facility (OLI) Oliktok Point, Alaska; AMF3 (M1)*. Atmospheric Radiation Measurement (ARM) user facility Data Center: Oak Ridge, Tennessee, USA. Data set accessed 2018-04-03 at http://www.archive.arm.gov/discovery/#v/results/s/fdsc::met. https://doi.org/10.5439/1025220

Laing, J. R., Hopke, P. K., Hopke, E. F., Husain, L., Dutkiewicz, V. A., Paatero, J., & Viisanen, Y. (2013). Long-term trends of biogenic sulfur aerosol and its relationship with sea surface temperature in Arctic Finland. *Journal of Geophysical Research: Atmospheres*, *118*, 11,770–11,776. https://doi.org/10.1002/2013JD020384

Leaitch, W. R., Sharma, S., Huang, L., Toom-Sauntry, D., Chivulescu, A., Macdonald, A. M., et al. (2013). Dimethyl sulfide control of the clean summertime Arctic aerosol and cloud. *Elementa: Science of the Anthropocene*, *1*. http://doi.org/10.12952/journal.elementa.000017

Leck, C., Norman, M., Bigg, E. K., & Hillamo, R. (2002). Chemical composition and sources of the high Arctic aerosol relevant for cloud formation. *Journal of Geophysical Research*, *107*(D12). https://doi.org/10.1029/2001JD001463

Leck, C., & Persson, C. (1996). Seasonal and short-term variability in dimethyl sulfide, sulfur dioxide and biogenic sulfur and sea salt aerosol particles in the arctic marine boundary layer during summer and autumn. *Tellus Series B: Chemical and Physical Meteorology*, *48*(2), 272–299. https://doi.org/10.3402/tellusb.v48i2.15891

Li, H., Pan, D., Wang, D., Gong, F., Bai, Y., He, X., et al. (2019). The impact of summer Arctic cyclones on chlorophyll-a concentration and sea surface temperature in the Kara Sea. *IEEE Journal of Selected Topics in Applied Earth Observations and Remote Sensing*, *12*(5), 1396–1408. https://doi.org/10.1109/JSTARS.2019.2910206

Li, S. M., & Barrie, L. A. (1993). Biogenic sulfur aerosol in the Arctic troposphere: 1. Contributions to total sulfate. *Journal of Geophysical Research*, *98*(D11), 20,613–20,622. https://doi.org/10.1029/93JD02234

Li, S. M., Barrie, L. A., & Sirois, A. (1993). Biogenic sulfur aerosol in the Arctic troposphere: 2. Trends and seasonal variations. *Journal of Geophysical Research*, *98*(D11), 20,623–20,631. https://doi.org/10.1029/93JD02233

Martin, M., Chang, R., Sierau, B., Sjogren, S., Swietlicki, E., Abbatt, J. P., et al. (2011). Cloud condensation nuclei closure study on summer arctic aerosol. *Atmospheric Chemistry and Physics*, *11*, 11,335–11,350. https://doi.org/10.5194/acp-11-11335-2011

May, N., Quinn, P., McNamara, S., & Pratt, K. (2016). Multiyear study of the dependence of sea salt aerosol on wind speed and sea ice conditions in the coastal Arctic. *Journal of Geophysical Research: Atmospheres*, *121*, 9208–9219. https://doi.org/10.1002/2016JD025273

McFiggans, G., Artaxo, P., Baltensperger, U., Coe, H., Facchini, M. C., Feingold, G., et al. (2005). The effect of physical and chemical aerosol properties on warm cloud droplet activation. *Atmospheric Chemistry and Physics*, *6*, 2593–2649. https://doi.org/10.5194/acp-6-2593-2006

Mungall, E. L., Croft, B., Lizotte, M., Thomas, J. L., Murphy, J. G., Levasseur, M., et al. (2016). Dimethyl sulfide in the summertime Arctic atmosphere: Measurements and source sensitivity simulations. *Atmospheric Chemistry and Physics*, *16*, 6665–6680. https://doi.org/10.5194/acp-16-6665-2016

Mungall, E. L., Wong, J. P., & Abbatt, J. P. (2018). Heterogeneous oxidation of particulate methanesulfonic acid by the hydroxyl radical: Kinetics and atmospheric implications. *ACS Earth Space Chemistry*, *1*, 48–55. https://doi.org/10.1021/acsearthspacechem.7b00114

NASA Goddard Space Flight Center, Ocean Ecology Laboratory, Ocean Biology Processing Group (2018). *Visible and Infrared Imager/Radiometer Suite (VIIRS) chlorophyll data; 2018 reprocessing*. Greenbelt, MD, USA: NASA OB.DAAC. https://doi.orgdata/10.5067/NPP/VIIRS/L3B/CHL/2018. Accessed on 07/31/2020

Nilsson, E. D., & Leck, C. (2002). A pseudo-Lagrangian study of the sulfur budget in the remote Arctic marine boundary layer. *Tellus Series B: Chemical and Physical Meteorology*, *54*(3), 213–230. https://doi.org/10.3402/tellusb.v54i3.16662

Norman, A., Barrie, L., Toom-Sauntry, D., Sirois, A., Krouse, H., Li, S., & Sharma, S. (1999). Sources of aerosol sulphate at Alert: Apportionment using stable isotopes. *Journal of Geophysical Research*, *104*(D9), 11,619–11,631. https://doi.org/10.1029/1999JD900078

O'Dwyer, J., Isaksson, E., Vinje, T., Jauhiainen, T., Moore, J., Pohjola, V., et al. (2000). Methanesulfonic acid in a Svalbard ice core as an indicator of ocean climate. *Geophysical Research Letters*, *27*(8), 1159–1162. https://doi.org/10.1029/1999GL011106

Osman, M. B., Das, S. B., Trusel, L. D., Evans, M. J., Fischer, H., Grieman, M. M., et al. (2019). Industrial-era decline in subarctic Atlantic productivity. *Nature*, *569*(7757), 551–555. https://doi.org/10.1038/s41586-019-1181-8

Pandis, S. N., Russell, L. M., & Seinfeld, J. H. (1994). The relationship between DMS flux and CCN concentration in remote marine regions. *Journal of Geophysical Research*, *99*(D8), 16,945–16,957. https://doi.org/10.1029/94JD01119

Park, K., Kim, I., Choi, J.-O., Lee, Y., Jung, J., Ha, S.-Y., et al. (2019). Unexpectedly high dimethyl sulfide concentration in high-latitude Arctic sea ice melt ponds. *Environmental Science: Processes & Impacts*, *21*(10), 1642–1649. https://doi.org/10.1039/C9EM00195F

Park, K.-T., Jang, S., Lee, K., Yoon, Y. J., Kim, M.-S., Park, K., et al. (2017). Observational evidence for the formation of DMS-derived aerosols during Arctic phytoplankton blooms. *Atmospheric Chemistry and Physics*, *17*(15), 9665–9675. https://doi.org/10.5194/acp-17-9665-2017

Petters, M., & Kreidenweis, S. (2007). A single parameter representation of hygroscopic growth and cloud condensation nucleus activity. *Atmospheric Chemistry and Physics*, *7*(8), 1961–1971.

Polissar, A., Hopke, P., Paatero, P., Kaufmann, Y., Hall, D., Bodhaine, B., et al. (1999). The aerosol at Barrow, Alaska: Long-term trends and source locations. *Atmospheric Environment*, *33*(16), 2441–2458. https://doi.org/10.1016/S1352-2310(98)00423-3

Pratt, K. A. (2016). *Aerosol mass spectrometer (aerosmassspec). Aug. 2016–Sept. 2016. ARM Mobile Facility (OLI) Oliktok Point, Alaska; AMF3 (M1)*. Oak Ridge, Tennessee, USA: Atmospheric Radiation Measurement (ARM) user facility Data Center. https://adc.arm.gov/discovery/#v/results/s/s::summertime%20aerosol

Pratt, K. A., Mayer, J. E., Holecek, J. C., Moffet, R. C., Sanchez, R. O., Rebotier, T. P., et al. (2009). Development and characterization of an aircraft aerosol time-of-flight mass spectrometer. *Analytical Chemistry*, *81*(5), 1792–1800. https://doi.org/10.1021/ac801942r

Pratt, K. A., & Prather, K. A. (2009). Real-time, single-particle volatility, size, and chemical composition measurements of aged urban aerosols. *Environmental Science & Technology*, *43*(21), 8276–8282. https://doi.org/10.1021/es902002t

Qin, X., Pratt, K. A., Shields, L. G., Toner, S. M., & Prather, K. A. (2012). Seasonal comparisons of single-particle chemical mixing state in Riverside CA. *Atmospheric Environment*, *59*, 587–596. https://doi.org/10.1016/j.atmosenv.2012.05.032

Quinn, P., Bates, T., Schulz, K., & Shaw, G. (2009). Decadal trends in aerosol chemical composition at Barrow, Alaska: 1976–2008. *Atmospheric Chemistry and Physics*, *9*(22), 8883–8888.

Quinn, P., Coffman, D., Kapustin, V., Bates, T., & Covert, D. (1998). Aerosol optical properties in the marine boundary layer during the First Aerosol Characterization Experiment (ACE 1) and the underlying chemical and physical aerosol properties. *Journal of Geophysical Research*, *103*(D13), 16,547–16,563. https://doi.org/10.1029/97JD02345

Quinn, P., Miller, T., Bates, T., Ogren, J., Andrews, E., & Shaw, G. (2002). A 3-year record of simultaneously measured aerosol chemical and optical properties at Barrow, Alaska. *Journal of Geophysical Research*, *107*(D11). https://doi.org/10.1029/2001JD001248

Rempillo, O., Seguin, A. M., Norman, A. L., Scarratt, M., Michaud, S., Chang, R., et al. (2011). Dimethyl sulfide air-sea fluxes and biogenic sulfur as a source of new aerosols in the Arctic fall. *Journal of Geophysical Research*, *116*, D00S04. https://doi.org/10.1029/2011JD016336

Renaut, S., Devred, E., & Babin, M. (2018). Northward expansion and intensification of phytoplankton growth during the early ice-free season in Arctic. *Geophysical Research Letters*, *45*, 10,590–10,598. https://doi.org/10.1029/2018GL078995

Rolph, G., Stein, A., & Stunder, B. (2017). Real-time environmental applications and display system: Ready. *Environmental Modelling & Software*, *95*, 210–228. https://doi.org/10.1016/j.envsoft.2017.06.025

Salmi, T., Määttä, A., Anttila, P., Ruoho-Airola, T., & Amnell, T. (2002). *Detecting trends of annual values of atmospheric pollutants by the Mann-Kendall test and Sen's slope estimates—The Excel template application MAKESENS*, Finnish Meteorological Institute, Publications on Air Quality.

Sen, P. K. (1968). Estimates of the regression coefficient based on Kendall's tau. *Journal of the American Statistical Association*, *63*(324), 1379–1389.

Serreze, M., Walsh, J., Chapin, F. S., Osterkamp, T., Dyurgerov, M., Romanovsky, V., et al. (2000). Observational evidence of recent change in the northern high-latitude environment. *Climatic Change*, *46*(1–2), 159–207.

Serreze, M. C., & Barrett, A. P. (2008). The summer cyclone maximum over the central Arctic Ocean. *Journal of Climate*, *21*(5), 1048–1065. https://doi.org/10.1175/2007JCLI1810.1

Sharma, S., Andrews, E., Barrie, L., Ogren, J., & Lavoué, D. (2006). Variations and sources of the equivalent black carbon in the high Arctic revealed by long-term observations at Alert and Barrow: 1989–2003. *Journal of Geophysical Research*, *111*, D14208. https://doi.org/10.1029/2005JD006581

Sharma, S., Barrie, L. A., Magnusson, E., Brattström, G., Leaitch, W., Steffen, A., & Landsberger, S. (2019). A factor and trends analysis of multidecadal lower tropospheric observations of Arctic aerosol composition, black carbon, ozone, and mercury at Alert, Canada. *Journal of Geophysical Research: Atmospheres*, *124*, 14,133–14,161. https://doi.org/10.1029/2019JD030844

Sharma, S., Chan, E., Ishizawa, M., Toom-Sauntry, D., Gong, S., Li, S., et al. (2012). Influence of transport and ocean ice extent on biogenic aerosol sulfur in the Arctic atmosphere. *Journal of Geophysical Research*, *117*, D12209. https://doi.org/10.1029/2011JD017074

Simmonds, I., & Rudeva, I. (2012). The great Arctic cyclone of August 2012. *Geophysical Research Letters*, *39*, L23709. https://doi.org/10.1029/2012GL054259

Simmonds, I., & Rudeva, I. (2014). A comparison of tracking methods for extreme cyclones in the Arctic basin. *Tellus A: Dynamic Meteorology and Oceanography*, *66*(1), 25252. https://doi.org/10.3402/tellusa.v66.25252

Song, X.-H., Hopke, P. K., Fergenson, D. P., & Prather, K. A. (1999). Classification of single particles analyzed by ATOFMS using an artificial neural network, ART-2A. *Analytical Chemistry*, *71*(4), 860–865. https://doi.org/10.1021/ac9809682

Stein, A., Draxler, R. R., Rolph, G. D., Stunder, B. J., Cohen, M., & Ngan, F. (2015). NOAA's HYSPLIT atmospheric transport and dispersion modeling system. *Bulletin of the American Meteorological Society*, *96*(12), 2059–2077. https://doi.org/10.1175/BAMS-D-14-00110.1

Stocker, T. (2014). *Climate change 2013: The physical science basis: Working Group I contribution to the Fifth Assessment Report of the Intergovernmental Panel on Climate Change*. New York, NY: Cambridge University Press.

Sultana, C. M., Cornwell, G. C., Rodriguez, P., & Prather, K. A. (2017). FATES: A flexible analysis toolkit for the exploration of single-particle mass spectrometer data. *Atmospheric Measurement Techniques*, *10*(4), 1323–1334. https://doi.org/10.5194/amt-10-1323-2017

Tang, M., Guo, L., Bai, Y., Huang, R.-J., Wu, Z., Wang, Z., et al. (2019). Impacts of methanesulfonate on the cloud condensation nucleation activity of sea salt aerosol. *Atmospheric Environment*, *201*, 13–17. https://doi.org/10.1016/j.atmosenv.2018.12.034

Tang, M., Whitehead, J., Davidson, N., Pope, F., Alfarra, M., McFiggans, G., & Kalberer, M. (2015). Cloud condensation nucleation activities of calcium carbonate and its atmospheric ageing products. *Physical Chemistry Chemical Physics*, *17*(48), 32,194–32,203. https://doi.org/10.1039/C5CP03795F

Virkkula, A., Teinilä, K., Hillamo, R., Kerminen, V.-M., Saarikoski, S., Aurela, M., et al. (2006). Chemical composition of boundary layer aerosol over the Atlantic Ocean and at an Antarctic site. *Atmospheric Chemistry and Physics*, *6*(11), 3407–3421.

Wagenbach, D., Ducroz, F., Mulvaney, R., Keck, L., Minikin, A., Legrand, M., et al. (1998). Sea-salt aerosol in coastal Antarctic regions. *Journal of Geophysical Research*, *103*(D9), 10,961–10,974. https://doi.org/10.1029/97JD01804

Williams, K., Jones, A., Roberts, D., Senior, C., & Woodage, M. (2001). The response of the climate system to the indirect effects of anthropogenic sulfate aerosol. *Climate Dynamics*, *17*(11), 845–856.

Willis, M. D., Köllner, F., Burkart, J., Bozem, H., Thomas, J. L., Schneider, J., et al. (2017). Evidence for marine biogenic influence on summertime Arctic aerosol. *Geophysical Research Letters*, *44*, 6460–6470. https://doi.org/10.1002/2017GL073359

Withycombe, E., & Dulla, R. (2006). Alaska Rural Dust Control Alternatives. Report prepared for the Alaska Department of Environmental Conservation. Sacramento, CA, USA: Sierra Research Inc.

Yamagami, A., Matsueda, M., & Tanaka, H. L. (2017). Extreme Arctic cyclone in August 2016. *Atmospheric Science Letters*, *18*(7), 307–314. https://doi.org/10.1002/asl.757

Ye, P., Xie, Z., Yu, J., & Kang, H. (2015). Spatial distribution of methanesulphonic acid in the Arctic aerosol collected during the Chinese Arctic Research Expedition. *Atmosphere*, *6*(5), 699–712. https://doi.org/10.3390/atmos6050699

Zhang, J., Ashjian, C., Campbell, R., Hill, V., Spitz, Y. H., & Steele, M. (2014). The great 2012 Arctic Ocean summer cyclone enhanced biological productivity on the shelves. *Journal of Geophysical Research: Oceans*, *119*, 297–312. https://doi.org/10.1002/2013JC009301

Zwaaftink, C. G., Grythe, H., Skov, H., & Stohl, A. (2016). Substantial contribution of northern high-latitude sources to mineral dust in the Arctic. *Journal of Geophysical Research: Atmospheres*, *121*, 13,678–13,697. https://doi.org/10.1002/2016JD025482